GRAIN SIZE ANALYSIS OF SEDIMENTS FROM THE MINAS BASIN, NOVA SCOTIA- CONTROLS OF EROSION ON THE SEABED SEDIMENT TEXTURE

by

Monique Ruhl

Submitted in partial fulfilment of the requirements for the degree of Combined Honours Bachelor of Science in Earth Sciences and Oceanography

at

Dalhousie University
Halifax, Nova
April, 2016

Distribution License

DalSpace requires agreement to this non-exclusive distribution license before your item can appear on DalSpace.

NON-EXCLUSIVE DISTRIBUTION LICENSE

You (the author(s) or copyright owner) grant to Dalhousie University the non-exclusive right to reproduce and distribute your submission worldwide in any medium.

You agree that Dalhousie University may, without changing the content, reformat the submission for the purpose of preservation.

You also agree that Dalhousie University may keep more than one copy of this submission for purposes of security, back-up and preservation.

You agree that the submission is your original work, and that you have the right to grant the rights contained in this license. You also agree that your submission does not, to the best of your knowledge, infringe upon anyone's copyright.

If the submission contains material for which you do not hold copyright, you agree that you have obtained the unrestricted permission of the copyright owner to grant Dalhousie University the rights required by this license, and that such third-party owned material is clearly identified and acknowledged within the text or content of the submission.

If the submission is based upon work that has been sponsored or supported by an agency or organization other than Dalhousie University, you assert that you have fulfilled any right of review or other obligations required by such contract or agreement.

Dalhousie University will clearly identify your name(s) as the author(s) or owner(s) of the submission, and will not make any alteration to the content of the files that you have submitted.

If you have questions regarding this license please contact the repository manager at dalspace@dal.ca.

Grant the distribution license by signing and dating below.

_____ _____

Name of signatory Date

Table of Contents

TABLE OF TABLES

TABLE OF FIGURES

ABSTRACT

The Minas Basin of the Bay of Fundy in Nova Scotia is a dynamic macro-tidal system providing great potential for harnessing tidal power. Tidal power extraction would affect flow speeds, which in turn may alter sediment size on the seabed. Because sediment size is a fundamental determinant of benthic community structure, extraction of energy could affect habitats in the Basin. A previous study indicated that the sediment distribution within the Bay of Fundy is not in equilibrium with the maximum tidal bed shear stress [Gelati, 2012]. Based on comparison of stresses predicted by a 3-D ocean circulation model and measured sediment sizes, the study showed that the competent mean grain sizes within the Bay of Fundy are generally coarser than observed mean grain sizes, suggesting that bed shear stress is not the dominant determinant of sediment texture in the Bay of Fundy. This thesis examines an alternate hypothesis that seabed sediment texture of the Minas Basin is determined by the texture of sediments entering the Basin through erosion of the surrounding cliffs, and not by local seabed stresses exerted by tidal currents. The objectives of this study are to (1) determine the grain size distribution of onshore samples and (2) compare the mean grain sizes to those found within the Basin. To test this hypothesis, samples of bedrock, unconsolidated beach sediments, and till (N=56, 29, and 7, respectively) were collected from four locations around the Minas Basin and compared to seabed samples collected from the Basin (N=161) by others. Analysis of samples suggests that grain sizes of eroding cliffs are similar to the grain sizes within the Basin. This is interpreted to support the idea that sediment derived by erosion of surrounding cliffs overprints the seabed sediment texture. Therefore it is unlikely that changes in energy caused by in-stream tidal turbines would have a large effect on the size of sediments in the Basin.

ACKNOWLEDGEMENTS

Many thanks to all my friends and family who have offered support and encouragement and kept me laughing over the past year. I would like to acknowledge my supervisor Dr. Paul Hill for his insight and dedication to this project. I would also like to thank Dr. Lawrence Plug for providing guidance along the way, and for always asking the bigger picture questions.

CHAPTER 1 INTRODUCTION

1.1 Introduction

The Minas Basin, Nova Scotia, is a dynamic macro-tidal system that is home to many intertidal and benthic organisms, as well as many migratory birds. In addition to providing unique habitats, the Minas Basin also has potential for harnessing tidal power. It has the largest tidal range in the world and tidal currents of up to 5 m s^{-1} [Hasegawa et al., 2011]. Simulations of the effect of tidal power extraction predict a decrease in tidal range during extraction [Hasegawa et al., 2011]. Reduced energy of flow could cause a decrease in sediment size. Therefore, extraction of energy could affect habitats by altering sediment texture. Alternatively, if input of sediment into a basin is large, then sediment texture can be defined by texture of input rather than by energy of the flows within the basin. In order to address the effects of tidal power development on grain size distribution and benthic habitat, it is important to understand the dominant control on seabed sediment texture.

The objectives of this thesis are to (1) determine the grain size distribution of eroding cliffs and (2) compare the mean grain sizes to those found in the Minas Basin. These objectives are addressed by quantifying and comparing grain sizes of samples collected from onshore samples to grain sizes of cores of Basin sediments.

The structure of this thesis is as follows. Chapter 2 provides background. Chapter 3 outlines the methods used for collection, lab work, and statistical analysis of lab data. Chapter 4 presents the results on grain size distribution. Chapter 5 discusses the results in terms of the controls on sediment transport and texture and of the effect of tidal power on sediment texture within the Minas Basin. Lastly, Chapter 6 will conclude with an interpretation of sediment texture in the Minas Basin and suggest possibilities for future work.

CHAPTER 2 BACKGROUND

2.1 Sediment texture

The sediment texture of a system is defined by the erosional and depositional processes. Erosion is the removal and transport of sediment, whereas deposition is the transport and placement of sediment. The amount and size of sediment in a system is determined by the system's competence, capacity, and supply of sediment [Hickin, 1995]. The competent mean grain size is the largest particle that a flow is capable of moving [Baker and Ritter, 1975]. The capacity refers to the maximum amount of sediment of a given size that the system can transport. Transport capacity is the competence-limited sediment transport, which only occurs if the supply is non-limiting. The sediment supply is the amount of sediment available to be transported. When a system is in hydrodynamic equilibrium, the competent mean grain size, capacity, and sediment supply can be used to infer local hydraulic stresses or, conversely, to predict changes in grain size caused by changes in local hydraulic stresses.

Sediment texture that is in equilibrium with local hydrodynamic stresses can be described through the concept of competent mean grain size. At equilibrium, the largest observed mean grain size of the system is determined by the maximum shear stress on the seabed [Baker and Ritter, 1975]. The Shields diagram allows one to determine the shear stress necessary to mobilise a particle of a given size and density (figure 2-1). Figure 2-1 indicates regions of hydraulically smooth, transitional, and turbulent flow [Buffington and Montgomery, 1997]. Critical shear stress (τ_c) is plotted against the Reynolds number (Re^*_C), where: $\tau^*_{C50} = \tau_{C50}/((\rho_s - \rho)gD_{50})$) and $Re^*_C = (u^*_C D_{50})/v$. The variables ρ_s and ρ are densities of the sediment and seawater, g is gravitational acceleration, D_s is the sediment particle diameter of interest, $u*$is the critical shear velocity, and v is the kinematic viscosity.

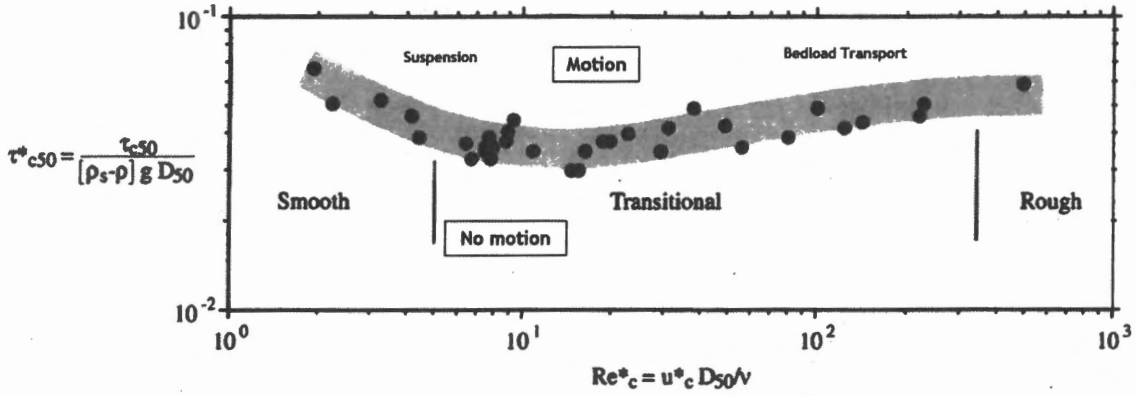

Figure 2-1 Shields diagram for sediment mixture at median grain size, D_{50} [modified by Buffington and Montgomery, 1997; annotated by author].

Stability of subaqueous bed sediment is dependent on the balance between forces which cause erosion and the resistive forces within the sediment [Grabowski et al., 2011]. Physical properties that can affect sediment erodibility are mean particle size, relative proportions of sand and mud, and water content. For instance, addition of clay to a sandy substrate increases resistance to erode by increasing cohesion. Biological properties affecting erodibility include burrows, feeding and egestion, and disturbance of the sediment surface [Grabowski et al., 2011]. The Hjülstrom diagram (figure 2-2a) plots empirical boundaries of when a given grain size will be entrained, transported, or deposited at a given velocity. The Postma diagram (figure 2-2b) plots the same boundaries at varying water contents.

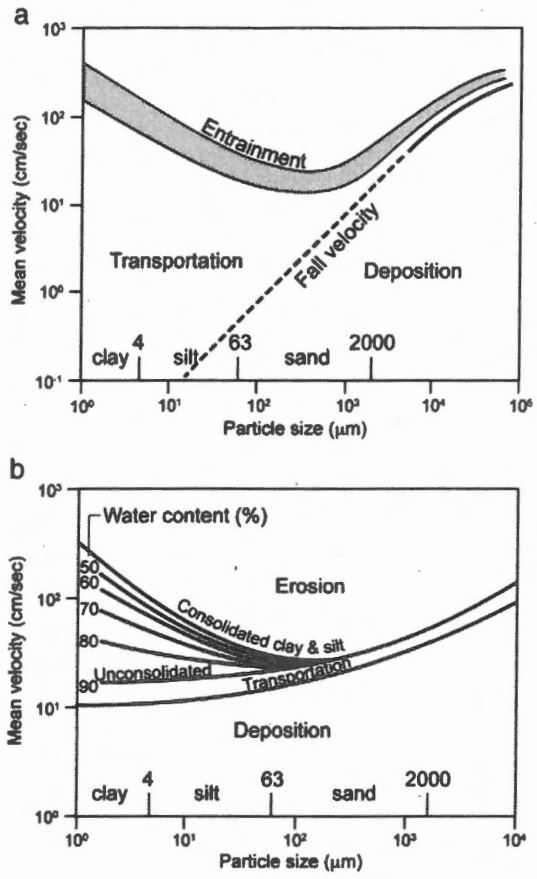

Figure 2-2 The (a) Hjülstrom and (b) Postma diagrams for erosion, transportation, and deposition of particle sizes at mean current velocity [from Grabowski et al., 2011].

Advances in numerical modelling have led to more complex and situational estimates on what causes sediments to erode, building from the original ideas proposed for stress and erosion at a given particle size. Porter-Smith et al. [2004] proposed a classification scheme to determine if tide, wave, or circulation currents are the primary cause of sediment erosion on a continental shelf. Tide-dominated locations are characterized where percentage of mobilisation of sediments by tidal currents exceeds two times the mobilisation caused by wave or circulation currents. Wave and circulation dominated are similarly defined. Wave-to-tidal ratio allows an assessment of the relative

importance of these mechanisms for mobilising bottom sediments. Porter-Smith et al. [2004] devised a six-part classification scheme: zero mobility, wave only, tide only, wave-dominated, tide-dominated, and mixed. Tide-only regions had a finer mean grain size and higher mean mud content than wave-only regions. This was explained by differences in sediment winnowing and trapping by waves and tides. Mud was trapped the most during flood and along shore tidal currents, and trapped the least during ebb tidal currents [Porter-Smith et al., 2004]. Mean grain size, sorting, and skewness follow trends that can be used to identify the direction of transport, as wells as sedimentary processes such as winnowing, selective deposition, and total deposition [McLaren, 1984].

Tidal currents have been identified globally as a renewable resource with potential for economic energy extraction [Neill et al., 2009]. In-stream tidal turbines work by intercepting kinetic energy from strong tidal currents, similar to wind turbines. A hydrodynamic model presented by Neill et al. [2009] found that a small amount of energy extracted from a tidal system can lead to significant impacts on sediment dynamics. For example, morphodynamic changes occurred up to 50 km from location of extraction. Furthermore the model shows that placement of in-stream turbines in relation to tidal asymmetry magnitudes had a large effect on sediment texture. Energy extraction from regions with high tidal asymmetry (where residual transport of sediment occurs in the flood or ebb direction), will have a much larger influence on broad sediment dynamics than energy extracted from regions with low tidal asymmetry [Neill et al., 2009]. Changes in sediment dynamics caused by a decrease in energy within a system may affect habitats of species that live in close association with the sea floor

2.1.1 Effect of seabed sediment texture on habitat

Benthic habitats may be distinguished based on sediment composition, grain size properties, transportation rate, and frequency of resuspension. On sediment-mantled continental shelves measurements of sediment mobility can provide a basis to predict the spatial and temporal distribution of benthic habitats [Porter-Smith et al., 2004]. Nutrient release from fine sand to mud substrate was recorded during plumes caused by dredging. Frequency of plumes were interpreted to be related to a significant enhancement of species richness and abundance of benthic biota, i.e. fauna responding to increased resources [Poiner and Kennedy, 1984]. This suggests a link between the structures of infauna benthic communities and episodic sediment erosion. A documented example of this is the copepod *Eurytemora herdmani*, which usually is most abundant in highly turbid waters, because it can maintain itself on particulate matter less than 60 μm in diameter [Daborn and Pennachetti, 1979].

Seabed sediment texture also influences larger organisms that live near the sea floor. For example, Atlantic cod was consistently found to be associated with cobble and gravel sized grains, because cod use the cobble substrate as nursery areas. Goosefish, hake fishes, and flatfish were commonly found in fine sand sized substrate, making use of a cover of sandy sediments to hide from prey [Methratta and Link, 2006]. Other factors that determine species selection for habitats are sediment mobility, waveforms, biogenic structures, and substrate relief. For example, skate species are found to be associated with flat sand [Methratta and Link, 2006].

Because of the well-documented relationship between marine species and sediment texture, the construction, operation, and decommissioning of in-stream tidal turbines will

likely have an effect on the habitat of benthic communities. Major consequences of installation and decommission phases are sediment removal and disturbance. Local sediment may be removed and smother a neighboring habitat. Resuspension of sediments high in organic matter may reduce the available dissolved oxygen concentration [Gill, 2015]. Habitat connectivity may be affected and could result in changes to community size and structure [Gill, 2005].

2.2 The Minas Basin

The Minas Basin is a semi-enclosed, macrotidal embayment located along the westernmost coast of Nova Scotia. It is subdivided into the main basin, which includes the Cornwallis, Avon, and Kennetcook River estuaries, and the easternmost Cobequid Bay, including the Salmon and Shubenacadie River estuaries. The Minas Passage narrowly connects the Minas Basin to the Bay of Fundy, then onwards to the Gulf of Maine and the Atlantic Ocean (figure 2-3).

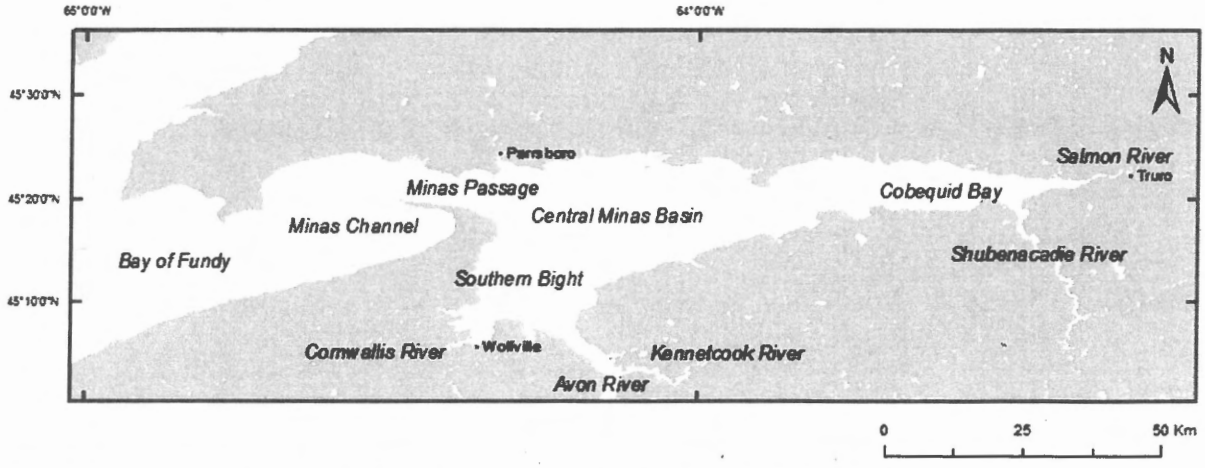

Figure 2-3 Regional map of Minas Basin. Shape files provided by Natural Resources Canada in GeoGratis as CanVec data.

2.2.1 Ecology of intertidal species

The Minas Basin supports many productive and diverse ecosystems [Brooks et al., 1999; Buzeta, 2014; Peer, 1980]. Large tidal range's and fast water flow promote nutrient cycling from coastal marshes, mudflats, and estuaries to the Basin and out into the Bay of Fundy. High productivity rates have been quantified in the intertidal mudflats due to this tidal flushing [Buzeta, 2014]. During the flood tide, nutrients and dissolved oxygen are transported over the mudflats to benthic organisms living in them. And waste is removed during the ebb tide. Additionally, over 40 species of fish have been found in the upper Bay of Fundy at high tide, where bottom feeders feed primarily on benthic invertebrates [Yeo and Risk, 1979].

Buzeta [2014] identified and reviewed the ecologically and biologically significant areas in the Bay of Fundy using data compiled from reports published by Fisheries and Oceans Canada. The following information was collected from the review. Large populations of *Barnea truncate*, or the Atlantic Mud-piddock clam, and the amphipod specie *Corophium volutator* live within mudflats in the Minas Basin. The Atlantic Mud-piddock is a warm water species unique only to the Minas Basin. *C.volutator* requires a unique combination of sand, silt, and clay for building their burrows. In addition to providing habitat for organisms that burrow in the substrate, the sediment texture of the Basin affects habitat suitability for algae. Kelp beds (*Laminaria spp.*), dulse, and coralline alga (*Corallina officinalis*) are found in waters near Cape Blomidon. Mudflats are significant areas for birds that feed on abundant *C.volutator*. This is particularly important during the fall migration of the Semipalmated Plover, as they rely on this food source to build fat in preparation for migration [Buzeta, 2014]. *C.volutator* population densities

within the substrate were at a maximum when the sediment was composed of 70% very fine sand, 30% silt and clay with a 20-25% water content [Peer, 1980].

The ecology of the Bay of Fundy is important to the commercial fishing industries of Eastern Canada and the USA. Cobscook Bay in the lower Bay of Fundy supports a large array of benthic organisms, including scallops, clams, mussels, and macroalgae. These are all sold commercially, and have large economical value [Brooks et al., 1999]. Increased productivity and diversity observed in Cobscook Bay is attributed to the large tides and associated exchange of nutrients when the tides flush the system [Brooks et al., 1999].

2.2.2 Regional geology and sediments

The Minas Basin is surrounded by eroding sandstone and basalt cliffs. The Fundy Group, comprised of McCoy Brook, North Mountain, Blomidon, and Wolfville Formations, is the most common. These rocks are Triassic to Jurassic in age and are primarily fluvial sourced sandstones and conglomerates, with minor tholeiitic basalts. The Port Hood Formation is found along the north coast of the Basin and is Carboniferous age. It is also interpreted as fluvial sandstones and conglomerates. The Windsor Group is located along the south coast of the Basin, and is composed of evaporates. The Windsor Group lies unconformably on the Carboniferous-aged Horton Group, which includes the Cheverie and Horton Bluff Formations consisting of predominantly fluvial sandstones and conglomerates. Geological classification is compiled by Keppie [2000]. A satellite image reveals high suspended sediment concentration at the head of the Basin [figure 2-4]. The

presence of extensive intertidal sand flats visible during low tide are further evidence of sedimentation and sediment movement within the Basin [Amos and Long, 1980].

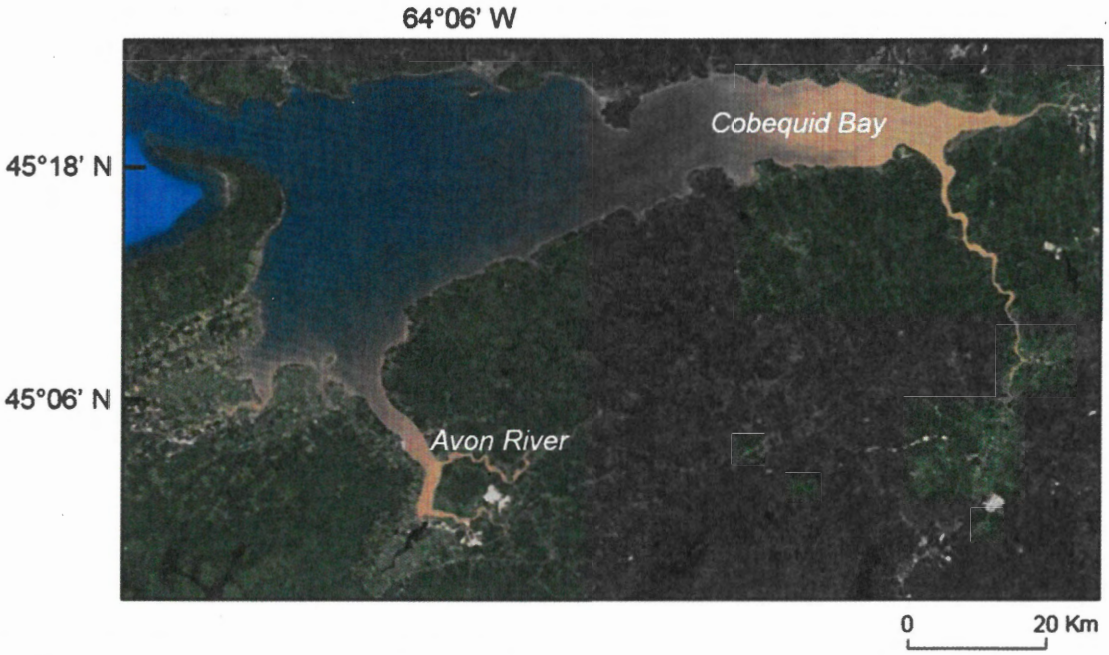

Figure 2-4 Satellite image of the Minas Basin. High turbidity waters are observed at the mouth of the Avon River and in Cobequid Bay (mouth of Salmon and Shubenacadie Rivers). Image obtained from Google Earth, 2015.

Mean grain size measurements of seabed samples collected by the Geological Survey of Canada and compiled by Li et al. [2015] show that the upper Bay of Fundy is dominated by medium to coarse sand, while the middle and lower Bay are covered by coarse sand and gravel. Within the Minas Basin system, coarsest sediment is found within Minas Channel, the northern coast of Minas Passage, and the central Minas Basin. The southern part of Minas Basin and Cobequid Bay are predominantly finer grained [Wu et al., 2011]. Based on calculations from 158 cliff height measurements and 20 recession measurements of cliff segments surrounding the Minas Basin, Amos and Long [1980] reported the largest volume of material entering the basin was from Five Islands and Cape Blomidon.

2.2.3 Tidal Setting

The Bay of Fundy has a semidiurnal tidal period. Tidal range varies from 2.4 m at the mouth of the Bay to 16.3 m in the Minas Basin, with a mean tidal range of 11.9 m [Amos and Long, 1980]. The natural tide period of the Bay of Fundy-Gulf of Maine system is slightly longer than the period of the dominant semidiurnal lunar (M_2) tide. The high tides are a result of the near-resonance between these two periods. There is a direct relationship between tidal amplitude and current speed [Amos and Long, 1980].

A maximum tidal current of 5 m s^{-1} occurs in the Minas Passage [Hasegawa et al., 2011]. Strong tidal currents are important for the mobilisation of bottom sediments. Models have shown that within the Minas Passage and Basin, tidal current shear velocities reach up to 10 cm s^{-1} and 5 cm s^{-1}, respectively [Li et al., 2015]. Tidal currents, as opposed to wave and circulation currents, have the largest effect on sediment mobilisation within the Minas Basin system. Wave shear velocity is typically 4 times less than tidal shear velocity. Sediment is mobilised by tidal currents greater than 30% of the time over most of the Bay of Fundy and 100% of the time in the Minas Passage. Comparatively, sediment is mobilised by waves only in shallow waters at the immediate coast [Li et al., 2015].

2.2.4 Previous Work: Implications of tidal power

Focus on the Minas Basin sediment texture and transport began in the late 1970s as a result of new tidal energy proposals to install tidal barrages. Installation was predicted to reduce circulation and cause deposition of sand around the barrages and permanent deposition of mud on the intertidal flats [Yeo and Risk, 1979]. Extraction of tidal energy was linked to a reduction in total primary productivity due to a decrease in efficiency of tidal flushing of nutrients and waster [Yeo and Risk, 1979]. Amos and Long [1980] created

a sediment budget from a simple input-output schematic model. Minas Basin inputs are (1) surrounding eroding cliffs, (2) rivers draining into the Basin, (3) seabed re-working, and (4) transport from the outer Bay of Fundy through the Minas Passage. And output of sediments from the Basin was through the Minas Passage. Cliff recession rates were measured from aerial photographs for 1939 to 1964 at 105 different sites. Mean recession was 0.55 m y^{-1}, with maximums of 1.5 m y^{-1} and 1.6 m y^{-1} at Five Islands and the north shore of Cobequid Bay, respectively. An estimated 4.8×10^6 m^3 y^{-1} of sediment was input into the Basin, where 58% was sand, 35% silt, and 7% coarser material.

Since then, advances in technology have shifted the focus from tidal dams or barrages to in-stream tidal turbines. Current research is now focused on installation of in-stream tidal turbines in the Minas Basin [Karsten et al., 2008; Wu et al., 2011; Hasewaga et al., 2011; Ashall et al., 2016]. Recent studies have used numerical models to investigate relationships between tidal forces, sediment mobility, and transport paths. Karsten et al. [2008] predicted that a maximum of 7 GW of power could be extracted from the Minas Basin, resulting in a 36% decrease in tidal amplitude. A less ambitious extraction scenario of 2.5 GW would not have large effects on the far-field tidal amplitudes. A maximum tidal current of 5 m s^{-1} was predicted for the Minas Passage and ~2 m s^{-1} within the Minas Basin [Li et al., 2015]. Using similar models, changes in sediment transport and distribution caused by changes in tidal energy have been predicted.

Within the Minas Basin system, sediments are transported predominantly as bedload, rather than suspended load. Bedload transport is most active in the Minas Channel, Minas Passage, and Cobequid Bay [Wu et al., 2011]. A maximum bedload

transport rate[1] of 2 kg m^{-1} s^{-1} was determined in the western Minas Passage, compared to 0.01 kg m^{-1} s^{-1} in open coastal waters. Suspended load transport rate in the Minas Channel and Passage is ~0.1 kg m^{-1} s^{-1}, and only 0.01 kg m^{-1} s^{-1} in the central part of the Basin. A comparison of the distribution of observed bottom sediment grain size and modelled shear stress, indicates a relationship between high stress and coarser grain size in the Minas Passage and northern Minas Channel. However, fine sediments observed in the central Basin were not associated with low shear stress levels [Wu et al., 2011]. The model by Wu et al. [2011] overestimated the bedload transport rate flux within the Basin. Similarly, Gelati [2012] calculated that competent mean grain sizes within the Bay of Fundy are generally coarser than observed mean grain size. This was interpreted as the observed seabed texture is not in equilibrium with the maximum tidal bed shear stress.

R^2 plots by Gelati [2012], of competent mean phi grain size against observed mean phi grain size show data points below the 1:1 line for locations within the Bay of Fundy and the Minas Basin. Illustrating a competent mean grain size coarser than observed mean grain size. Additionally a proportional relationship between increasing stress and increasing grain size did not exist for the Bay of Fundy. Conversely, results for the Gulf of Maine show an increase in grain size with increase tidal bed shear-stress, as well as particles following a calculated competent mean grain size better than those within the Bay of Fundy. Competent mean grain size was computed using maximum modeled tidal bed shear stress and a corresponding critical erosion value. Observed mean grain size was determined from multiple data sets.

---

[1] Sediment transport rate was defined as the total mass transport of sediment per unit length of lateral cross section, perpendicular to the vector transport, therefore units are kg s^{-1} m^{-1}. This quantity was integrated along a transect of interest to give total transport through section.

For competent and observed grain sizes to match, the following assumptions must hold [Gelati, 2012]: (1) Tidal near-bed currents, as opposed to wave, are the dominant source of bed-shear stress, (2) sediment supply of grain sizes smaller than competence does not exceed transport capacity, (3) all grains are resuspended under maximum bed shear stress, and (4) there is residual near-bed flow. Therefore, using this approach, if tidal bed shear stress changes, everything else being equal, sediment texture will change accordingly. Gelati [2012] determined that an absence of residual flow or frequent transport of sand are not the source of disagreement between competent and observed grain size. It is most likely that a high input of sediment supply finer than the competent mean grain size is the main source of disagreement. It is estimated that 2.72×10^{6} m^3 a^{-1} of mainly sand sized material is being eroded from adjacent cliffs into the Basin, compared to $\sim5\times10^{4}$ m^3 a^{-1} of input by fluvial sediment [Amos and Long, 1980]. This thesis examines an alternate hypothesis proposed by Gelati [2012], that sediment supply from erosion of the adjacent cliffs is the likely cause of the disagreement between competent and observed mean grain size. I will investigate the relationship between seabed sediment texture in the Minas Basin and the grain size distribution of material supplied from erosion of adjacent cliffs.

CHAPTER 3 METHODS

3.1 Onshore Sample selection

Sampling took place over three field days in July and August 2015. Samples collected by Fernandes and Hill in July 2014 are also used for data analysis. Figure 3-1 provides a map of the locations of samples from GPS measurements. A total of 92 samples collected from bedrock (56), unconsolidated beach sediments (29), and till (7) are used for grain size distribution analysis. Samples spaced approximately 175 m apart were collected with a trowel and placed in Ziploc bags.

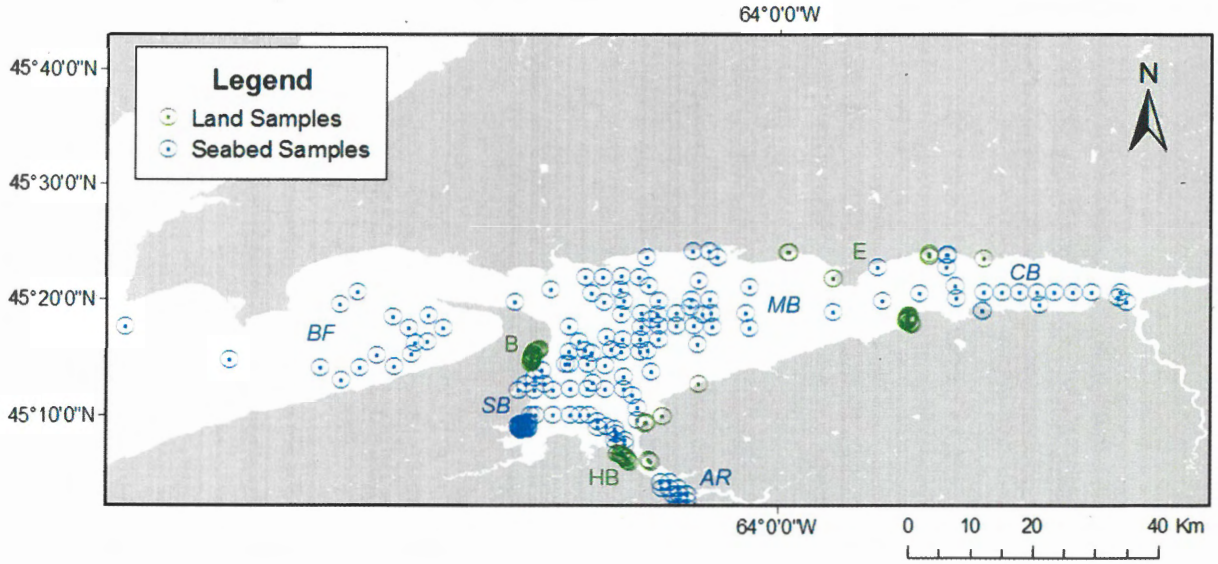

Figure 3-1 Distribution of samples collected on the shores of and within the Minas Basin, NS.

3.1.1 Seabed Samples

Seabed sediment distribution analysis was done on samples collected by Bedford Institution of Oceanography (BIO) scientists in June 2013. Ninety-two nearshore samples were collected using Van Veen and Ekman grabs, as well as, sixty-nine deep-water (> 30

to 40 m depth) samples using a Video Grab instrument by the crew on the *CGS Hudson*. Samples were dried, crushed, and sieved at the BIO.

3.2 Sieve Analysis

Approximately 150 grams from each sample was weighed and dried in an oven for at least 24 hours. Dried samples were weighed, crushed, and washed through a 63 μm sieve. After wet-sieving, samples were dried and re-weighed to determine the proportion of sediments less than 63 μm. The remaining sediment was put through a standard sieve set ranging from 2 mm to 63 μm and shaken for 20 minutes. Fraction retained on each sieve was recorded.

3.3 Data Analysis

The data obtained from sieving was used to create graphical representations of weight distribution of samples and to compare with the distribution for seabed samples. Mean and standard deviation were calculated as described by Tanner [1995]. Tables 3-1 and 3-2 provide verbal classification of mean and standard deviation, adopted from Folk and Ward [1957].

Table 3-1 Textural class names of grain sizes [Folk and Ward, 1957]

Texture	Φ Size	Metric size (μm)
Gravel	< -1	>2000
Very coarse sand	-1 to 0	2000-1000
Coarse sand	0 to 1	1000-500
Medium sand	1 to 2	500-250
Fine sand	2 to 3	250-125
Very fine sand	3 to 4	125-63
Silt and clay	>4	<63

Table 3-2 Geometric sorting verbal classification [Folk and Ward, 1957]

Sorting	Value
Very well sorted	<0.35
Well sorted	0.35-0.50
Moderately well sorted	0.50 to 0.70
Moderately sorted	0.70 to 1.00
Poorly Sorted	1.00 to 2.00

CHAPTER 4 RESULTS

4.1 Grain size distribution of total sieved sample

Mean retained weight percent of gravel (< -1 ϕ), sand (-1 to 4 ϕ), and silts and clays (> 4 ϕ) were plotted for each sediment source (fig 4-1). Each sediment source, except the glacial tills and deep-water Basin samples, was dominated by sand. Till had approximately equal proportions of sand and mud (silt and clay) with a small gravel fraction, and the deep-water sediments from the Basin had approximately equal percentages of gravel and sand with a small mud fraction. Gravel content was less than 20% for all but the deep-water sediments. Silt and clay percentages decreased distally from onshore to offshore. Figure 4-2 plots each sediment type on a gravel-sand-mud trigon diagram. Based on this classification scheme, deep-water sediments plot within the gravel corner, till plot within the mud corner, and beach, cliff, and nearshore samples plot in the sand corner.

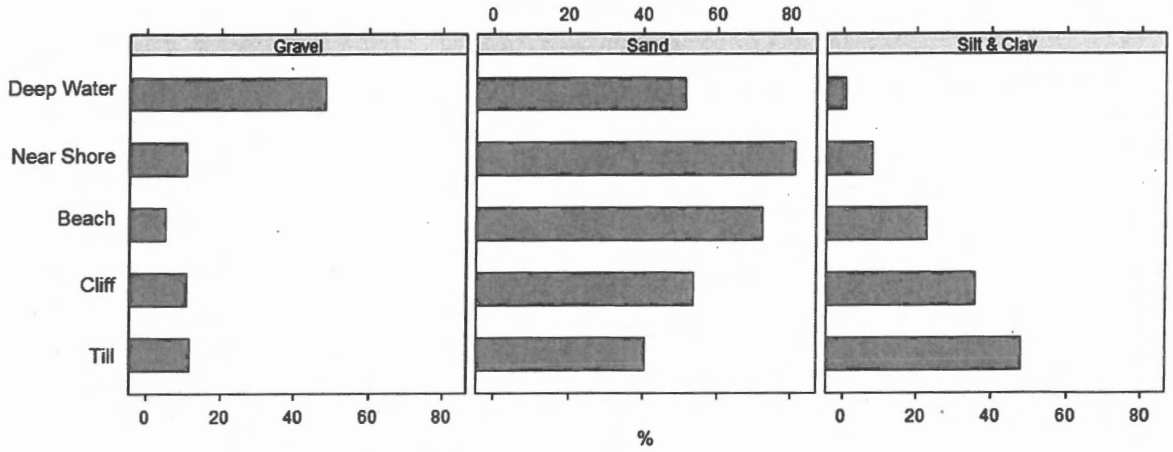

Figure 4-1 Average percent distribution of gravel, sand, and silt and clay sized particles for till (n=7), cliff (n=56), beach (n=29), near shore (92), and deep-water (n=69) sediment samples.

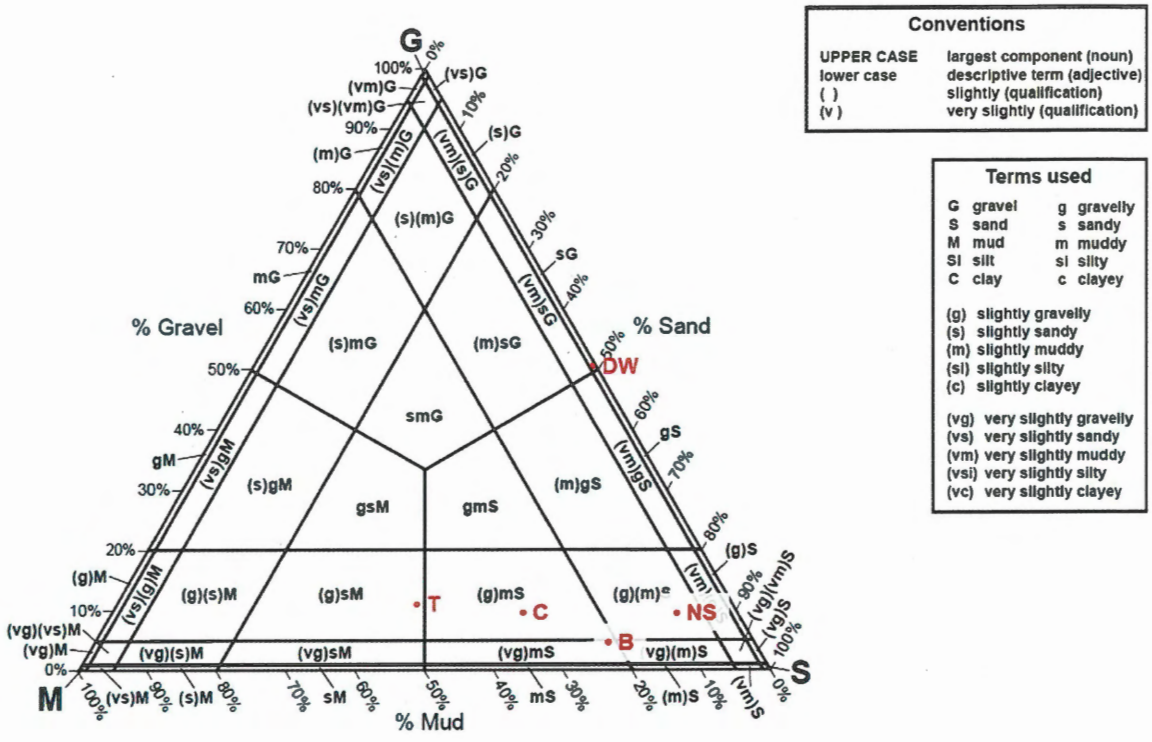

Figure 4-2 Average percent distribution of gravel, sand, and silt and clay sized particles for each sediment type plotted on gravel-sand-mud trigon [Blott and Pye, 2001].

4.2 Grain Size Distribution of sand sized portion

The sand size portion of the grains were compared because that was the size of interest, as well as grains larger than gravel and smaller than mud were not constrained on either side. Figure 4-3 plots the sand grain size distribution of percent retained weight at each sieve. Highest percent retained weight of till occurred on the ~3.2 ϕ sieve at Blomidon and Horton Bluff, whereas at Economy Point most of the sediment was retained on the 4 ϕ sieve. Cliff sediment frequency distribution had a modal phi size less than till. At Blomidon and Hortons Economy point, sediment from the cliffs was retained primarily on the 3.0 ϕ sieve, whereas at Hortons Bluff it was distributed primarily on the 1.5 ϕ sieve. Most

common grain size of beach sediment sources was ~1.5 ϕ. Beach sediments present the most normal distribution of grain sizes. Till and cliff distributions are fine-skewed.

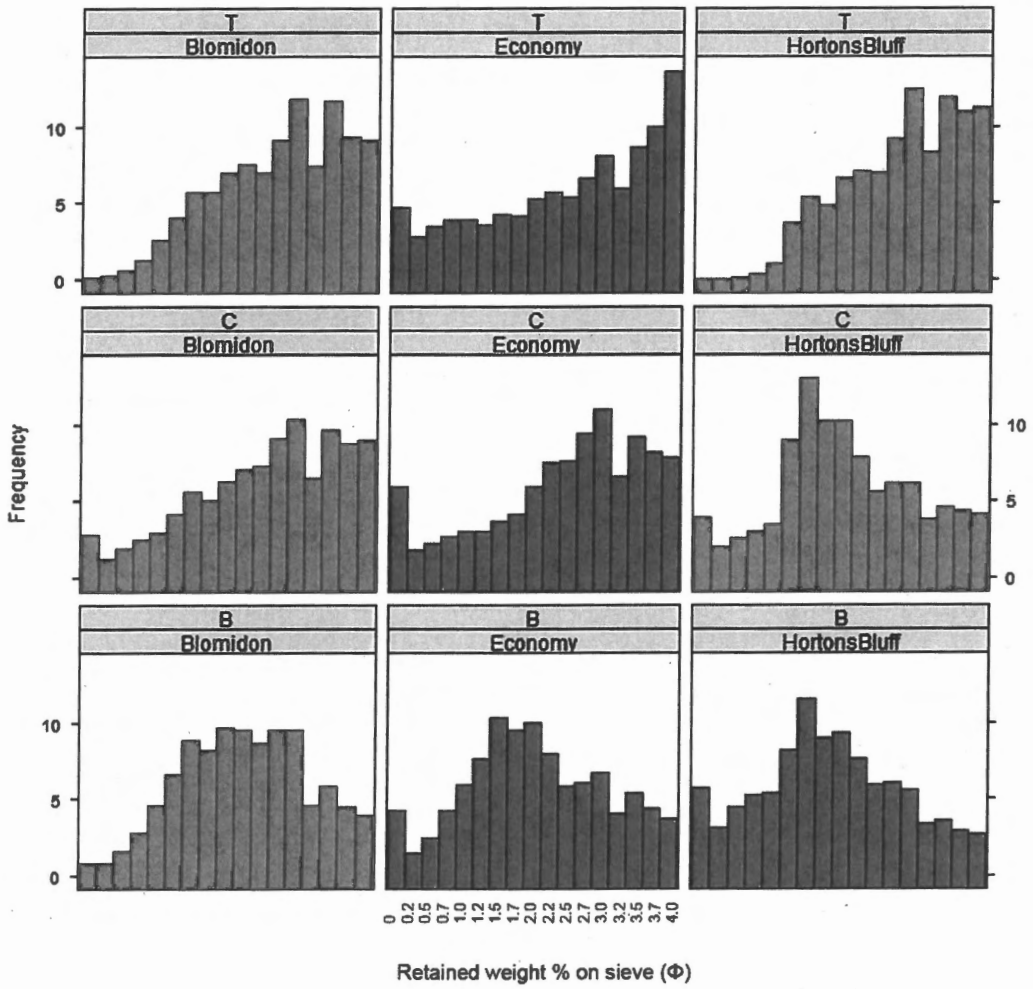

Figure 4-3 Frequency of average grain sizes of sand portion (-1 to 4 ϕ) of land samples by location. Data averaged over same number of samples as in figure 4-1.

Frequency of retained weight of sieves in the sand grain size range was plotted for near shore and deep-water sources, at each location (fig 4-4 and 4-5, respectively). Highest percent retained occurred on the 3.0 ϕ sieve in the Avon River and Southern Bight locations. Moving northwest in the Basin, the distribution coarsened to 2.0 ϕ in Cobequid Bay. Distribution of deep-water sediment sources show 2.0 ϕ as the modal grain size.

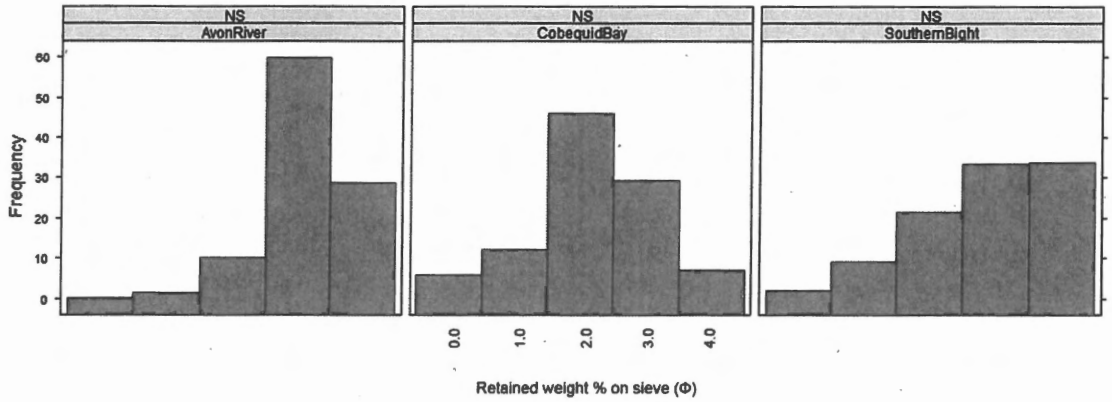

Figure 4-4 Frequency of average grain sizes of sand portion (-1 to 4 ϕ) of nearshore seabed samples by location. Data averaged over same number of samples as in figure 4.1.

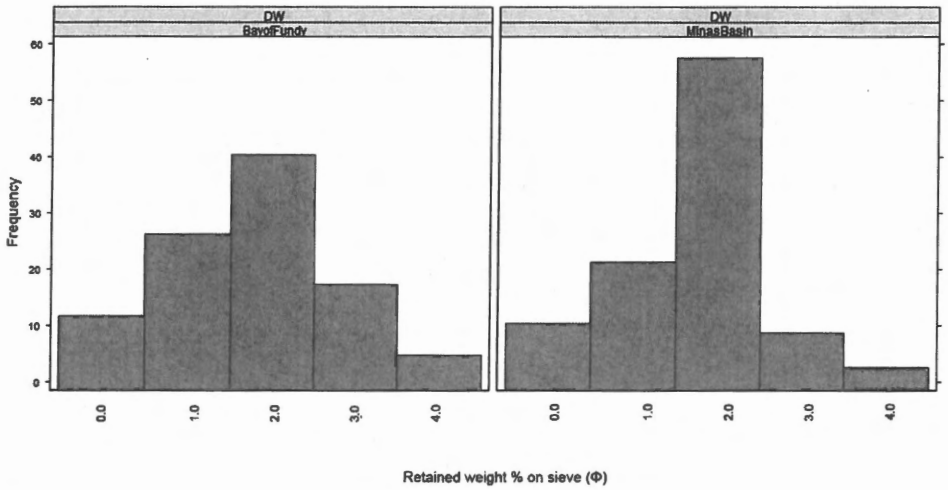

Figure 4-5 Frequency of average grain sizes of sand portion (-1 to 4 ϕ) of deep-water seabed samples by location. Data averaged over same number of samples as in figure 4.1.

Average size of land samples of the sand portion was fine sand, compared to medium sand from all seabed samples. Land samples were more sorted than seabed. Beach samples were the most sorted, followed by till, then deep-water, near shore, and least sorted was cliff. Figure 4-6 shows the distribution of means based on sediment source. Deep-water sediments have the coarsest grain size distribution. Cliff, beach, and nearshore medians are all ~2.25 ϕ size. Till has the finest distribution of mean grain size. Nearshore

and cliff sediments are widely distributed across ~1.0 to 3.5 ϕ size range, whereas the distribution of beach sediments is more constrained to 1.5 to 3.0 ϕ. Till and deep-water sediments are the only sources that do not overlap in grain size distribution. The medians of cliff, beach, and near shore sediment sources all plot within one another's mean distribution. Although silt and gravel amounts vary between location and sediment type, each distribution has a mean and median grain size in the sand size range.

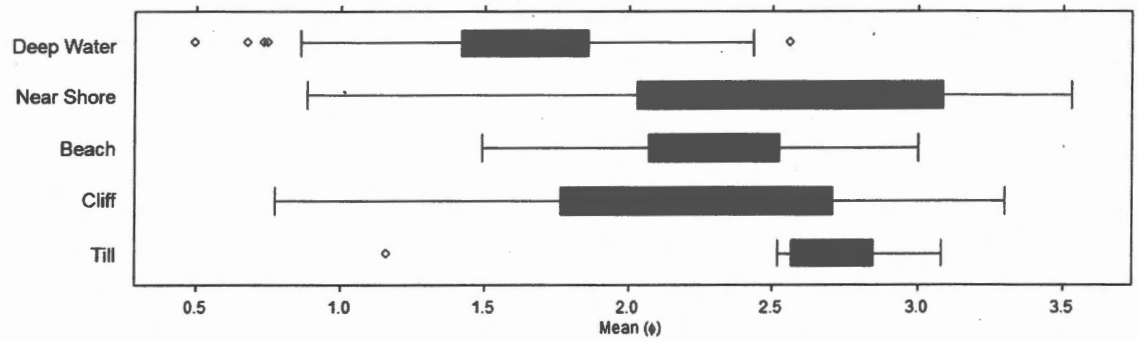

Figure 4-6 Boxplot of mean grain sizes for each sediment source. Left and right edges represent first and third quartiles, boxes middle lines represent the medians, whiskers represent values 1.5 times the respective interquartile distances, and open circles represent outliers.

4.3 Errors on sieving method

Sample B-13 was sieved five times to compute the standard error of one sample. This was compared to the standard error of a transect of beach sediment samples (13, 14, 17, 20, and 22). The sample standard deviation of B-13 was smaller than the sample standard deviation across five different locations. Because within sample variability is smaller than geographic variability among samples collected from the same beach, observed differences among samples indicate different conditions among sites rather than random variation caused by the sieving methodology.

CHAPTER 5 DISCUSSION

5.1 Controls on sediment transport

Within the Minas Basin system, there is a textural transition of sediments coarsening from onshore to offshore. The average phi size decreases from land to seabed samples. Data are in agreement with the characteristic sediment pattern observed at tide-dominated coasts. The decrease in percent silt and clay as shown in figure 4-1 is attributed to winnowing of fine sediments, rather than addition of coarser sized grains. A landward decrease in tidal energy tends to cause a landward fining of sediments along a tidal flat [Daidu et al., 2013].

Tides dominate sediment transport in the Minas Basin [Li et al., 2010; Wu et al., 2011; Swift, 1967; McLaren 1978]. The Basin has 360 km^2 of intertidal flats, concentrated in Cobequid Bay and the Southern Bight regions [Ashall et al., 2016]. Sediment sorting along a tidal flat is influenced by tidal currents [Zhou et al., 2014]. Beach sediments are most sorted, followed by till, deep-water, nearshore, and cliff sediments are the least sorted. Overall, seabed samples were more sorted than land. Gelati [2012] predicted a similar sorting value of 2.5 at the Southern Bight.

The eroded sediment from the cliffs is interpreted as the source of material for the beach, nearshore and deep-water environments. From cliff to beach, the percent of grains within the silt and clay size range decreases and sand-sized grain percent increases (figure 4-1). Where high tide reaches the cliff face, the beach directly below will have a lower silt and clay content than its source. Strong wave shear velocities remove the fine sediment and carry it in suspension offshore.

From beach to nearshore, there was an increase in very fine sand sized grains. Fine sediment is transported in suspension to the near shore environment or brought up and trapped in salt marshes (Proosdij et al., 2000). In addition to fines winnowed from the beach, the flood tide brings in suspended sediment from the basin to the tidal flats. During high tide slack water, clay sized particles settle onto the nearshore environment and become mixed with the coarser sediments [McLaren, 1984]. As the tides retreat some of the clay is removed, but most remains mixed with the other tidal flat sediments [McLaren, 1984]. The nearshore environment is a place for fine sand sediment accumulation because wave action is minimal compared to at the beach, and the water depth is shallow enough for the sediments to settle, as opposed to deep-water. Strongest tidal currents occur in deep-water, where accordingly the samples have the lowest silt and clay sized grains and the highest percent of gravel sized sediments.

Weak tidal currents in the lower mid-Bay of Fundy favour fine sediment accumulation and a wider distribution of sand and mud, whereas areas of strong tidal currents favour erosion of seabed [Wu et al., 2011]. In the Minas Basin, the spatial transition from mudflats to sand flats has been reported to occur close to where peak tidal stress first exceeds the erosion threshold for intertidally exposed muds [Friedrichs, 2011]. Mud can easily be transported to any part of the flat. But after deposition, cohesion increases the stress needed to surpass the erosion threshold [Friedrichs, 2011]. Figure 5-1 plots a textural transition along a tidal flat of shear stress against intertidal elevation [adapted from Amos 1995]. High elevations and mud accumulation are attributed to low values of peak bed shear stress, while lower elevations are defined by high peak bed shear stress and in the sand accumulation zone [Friedrichs, 2011]. This may explain the highest

percent abundance of very fine sand in the nearshore samples. Textural changes in grain size distribution from onshore to offshore, suggest that tides control the bedload and suspended load sediment transport within the Minas Basin.

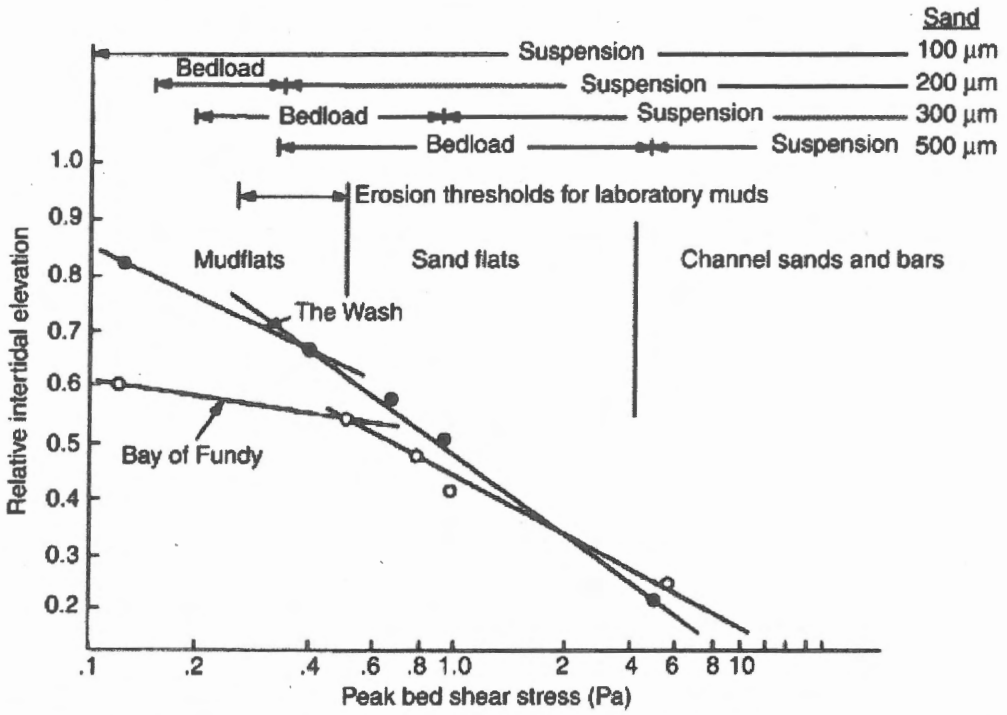

Figure 5-1 Peak bed shear stress and the location of mud-sand transition across tidal flats in the Minas Basin (bottom lines) from [Amos, 1995]. Modified by [Friedrichs, 2011] to show the erosion thresholds for laboratory muds and the transportation mode for sand.

From this analysis, it is interpreted that in the Minas Basin tides dominate sediment transport but they do not likely dominate sediment texture. The overall textural transition is overprinted by a finer sediment source than expected based on the tidal energy. Therefore the sediment texture is likely determined by the sediment texture entering the Minas Basin through erosion of adjacent cliffs.

5.2 Controls on sediment texture

In the Bay of Fundy, competent mean grain sizes are generally coarser than observed mean grain sizes [Gelati, 2012]. Three possibilities for a general disagreement between observed and competent are (1) lack of stress to remove sediments, (2) lack of supply of appropriate grain sizes available to be transported, and (3) overprinting of seabed texture by a source with a distribution finer than the competent grain size. As previously mentioned, the Bay of Fundy has the largest tidal range in the world, and tidal current speeds have been predicted up to 5 m s^{-1} in the Minas Passage (Hasegawa et al., 2011). As well as, the wide-spread presence of a residual near-bed tidal flow will move suspended sediments away from their original location of deposition [Gelati, 2012], suggesting it is unlikely that the Minas Basin is a transport limited system. The second possibility suggests that the Minas Basin would have to be a supply limited system. This is also unlikely because there is a wide distribution of grain sizes present in the Bay of Fundy to be transported [Gelati, 2012], entering as glacial, fluvial, or as eroded bedrock sources [Amos and Long, 1980]. Therefore the disagreement between observed and predicted mean grain size within the Bay of Fundy is likely caused by an abundant supply of sediment with an average grain size finer than that calculated by the critical shear stress.

Accordingly, in the following I will discuss the interpreted source of sediment and the implications of sediment supply on the overall textural transition, in regards to tidal power energy extraction.

5.2.1 Sediment source

Cliff sediment is primarily sand sized (figure 4-1). Cliffs are eroding at rates up to 2 m a^{-1} around the Minas Basin [Amos and Long, 1980]. Total volume of sediment from cliff erosion was estimated to be 3.09×10^6 m^3 a^{-1} [Amos and Long, 1980].

Figure 5-2 shows a map of cliff recessions rates by Amos and Long [1980] superimposed on a map of sample locations. Highest rates were recorded along the north shore, specifically at Five Islands, Economy Point, and around Cobequid Bay. These can be spatially correlated to land samples collected from Economy Point and seabed samples of the central Minas Basin and Cobequid Bay. The cliff samples of Economy are slightly fine-skewed, compared to the beach samples of Economy Point, which are centered on 1 and 2 ϕ. The distribution is similar to that of the Minas Basin deep-water samples, which are also centered on 1 and 2 ϕ. Port Hood fluvial sandstones are eroding along the north shore of Cobequid Bay. The seabed samples collected from the Bay were medium sand size on average. Therefore it is likely that the sand found within the Basin is derived from the cliffs.

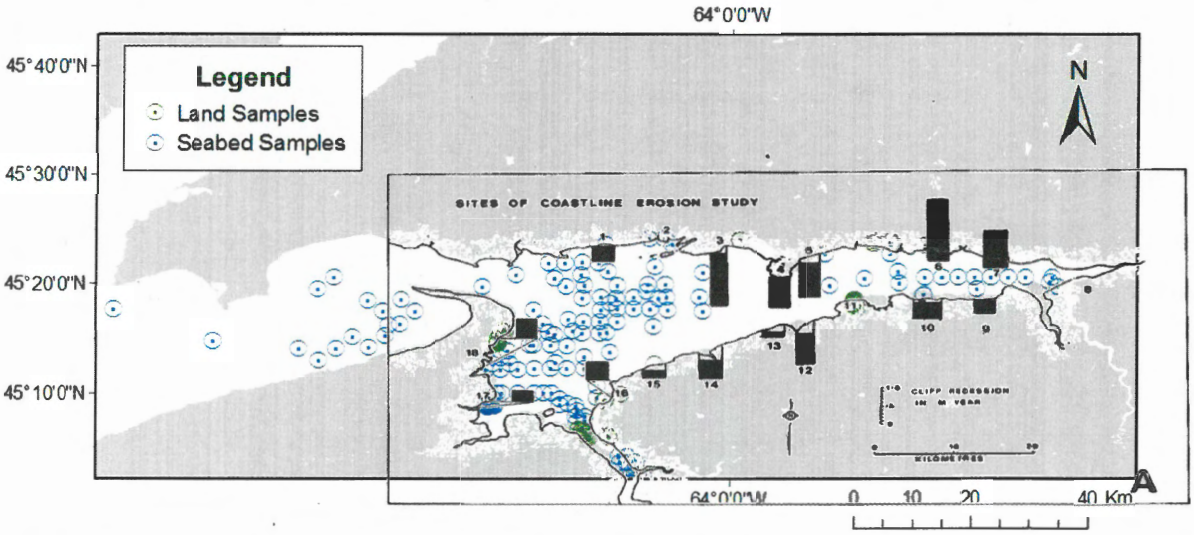

Figure 5-2 Sample locations overlain with cliff recession map (m a^{-1}) calculated by Amos and Long [1980].

Mean grain size of land samples was fine sand, whereas the mean grain size of seabed samples was medium sand. Till and deep-water sediments are the only environments whose distributions do not overlap (figure 4-6). Since the grain size distribution from the cliff samples is similar to the distribution of seabed sediments, I propose that the sediments eroding from adjacent the cliffs define the seabed sediment texture within the Minas Basin. Accordingly, I infer that the disagreement between maximum tidal bed shear stress and observed mean grain size is a result of an abundant supply of sediments finer than the competent grain size, i.e. sediment supply exceeds the energy of the system. Therefore when predicting changes resulting from tidal energy extracting from the Minas Basin, it is necessary to consider sediment texture as well as sediment transport. In order to predict changes to sediment transport and distribution, you first need to constrain the initial sediment texture.

5.2.2 Sediment supply: rate and magnitude

The seabed sediment texture is controlled by the texture of the cliffs because tidal energy is unable to remove sediment eroding from the adjacent cliffs into the Minas Basin. i.e. where sediment supply exceeds transport capacity, the seabed sediment distribution will be determined by the texture of sediment input, rather than hydraulic energy. The presence of large bed forms on the seafloor of the Minas Basin are evidence of abundant sand supply. Banner banks are a bedform that occurs when sediment supply is abundant and bedload transport is induced. These are observed off the coast of Cape Split [Todd et al., 2014]. Moreover, broad intertidal mud flats are formed from contributions of sediment derived from cliff erosion, coupled with seafloor erosion and sediment delivered by rivers [Todd et al., 2014]. These features provide evidence for a large volume and large rate of

sediment input in the sand size range to the Minas Basin. Suggesting that sediment supply is an important consideration when predicting changes to the hydrodynamic system of the Minas Basin.

When using models to predict influence of tidal power development on the sediment distribution within the Minas Basin, a question that needs to be asked is: how does the Minas Basin seabed surface adjust to changes in sediment supply and texture? Studies on river systems have tried to answer this question (Baker and Ritter, 1975; Jackson and Bechsta, 1984, Dietrich et al., 1989; Lisle et al., 1993; Ferrer-Boix and Hassan, 2014). There have been fewer experiments on sediment supply and transport capacity for coastal, tide-dominated systems.

Shear stress analysis can provide an easy way to estimate the competence of rivers to transport particles as bedload [Baker and Ritter, 1975]. The Shield's parameter is used more often than velocity because it is easier and more accurate to measure the depth of water column, dimensionless slope, and specific gravity of water, than the velocity of a river channel. Limitations arise when systems diverge from hydrodynamic equilibrium. Challenges which have been documented are changes in water depth, increased sediment supply as well as supply limited systems, and episodic supplies to a river channel. Flow mechanics differ depending on height of the water column [Baker and Ritter, 1975]. For instance, in deep flows the shear stresses needed to entrain particles may be greater than predicted by Shield's because there is little hydrodynamic lift [Baker and Ritter, 1975].

As well as changes in water depth, the influence of increased sand delivery on river channel velocity has been examined [Jackson and Beschta, 1984; Buffington and Montgomery, 1999]. The initial response of a channel to an increased supply of sand-sized

sediments is to reduce the surface roughness by fine-grained sediment deposition, which will in turn, increase flow velocity and bedload transport capacity [Jackson and Beschta, 1984; Buffington and Montgomery, 1999]. Therefore the bed surface texture represents a feedback between sediment supply rate and bedload transport, induced by changes in bed roughness and sediment availability. Furthermore, where transport capacity is overwhelmed by sediment supply selective entrainment of grain sizes will occur [Buffington and Montgomery, 1999]. Alternatively, when transport capacity exceeds sediment supply, the median grain size of the bed surface is coarser than the transported load [Dietrich et al., 1989; Lisle et al., 1993]. When an equilibrium between surface and bedload transport rate was reached, the surface became finer and better sorted [Dietrich et al., 1989].

Similarly, Ferrer-Boix and Hassan [2014] investigated how the bed surface adjusts to different sediment supplies and textures. In a flume experiment, fine material in a low flow sand-supplied run infiltrated the bed surface at the beginning, then remained on top once the near-surface pores were saturated. Therefore the surface coarsened then subsequently became finer. When the flow was increased, the bed surface coarsened regardless of the supply texture [Ferrer-Boix and Hassan, 2014]. These results are significant for gravel-bed stream subjected to episodic sediment inputs, where the frequency of sediment input may prevent the river from recovering or achieving equilibrium. Similar concepts have been applied to tidal regions [Friedrichs, 2011; Pritchard and Hogg, 2003].

When averaged over annual, or longer, timescales, tidal flat morphology will typically approximate a dynamic equilibrium with external forcing (sediment supply and

wave and tidal forcing). Assuming this equilibrium, dominance by tides results in a convex-up profile further favoured by increased sediment supply. However, surficial grain size responds to changes in energy more quickly than overall morphology can adjust, consequently leading towards a landward fining in surficial grain sizes [Friedrichs, 2011]. Pritchard and Hogg [2003] suggest that the morphology of mud flats depends strongly on the external supply of sediment to the system. In that, the gradient of the flat increased with increasing tidal range and decreased with a larger sediment supply.

From these laboratory flume experiments and numerical models, it becomes clear that the interplay between sediment supply and transport capacity affect the theoretical hydrodynamic equilibrium concepts used to predict changes in real settings.

For example, maximum bed shear stress is not a good predictor for largest grain size in the Avon River estuary because of the abundant supply of fine material [Lambiase, 1980]. The Shields' criterion failed to predict coarsest grain size at the estuary head because of hydraulic sorting. The coarse grain sizes that the strong currents are capable of transporting are excluded from the estuary head and fine sediments are present everywhere along the estuary. Sediment transport paths in the river result from sediment exchange between the estuary head and mouth, rather than the inverse relationship between mean grain size and current velocity [Lambiase, 1980]. Similarly, beaches along the southwestern Louisiana coast provide an example of a shoreline being loading with fine sediments from rivers. Here, the sediment supply exceeds the hydrodynamic energy so most of the deposited fines do not get winnowed out. It is interpreted that the system will eventually reach equilibrium once the river is diverted [Friedman, 1967].

Based on these experiments and real-world examples, the estimated balance between tidal bed shear stress and grain size texture in the Minas Basin should be re-evaluated. Using critical shear stress theory, competent mean grain size overestimates the mean grain size within the Bay of Fundy. The disagreement is primarily attributed to sediment supply in excess of transport capacity. When input of sediment into a basin is large, sediment texture can be defined by texture of input rather than by energy of the flows within the basin. However, there are other processes that may also contribute to the disagreement.

5.2.3 Other factors controlling sediment texture

Additional processes that may lead to observed grain sizes that are finer than competent mean grain sizes are cohesion of sediments, sediment trapping, and seasonal fluxes of sediment. For instance McLaren [1984] identified cohesion of fine sediments as the cause of fining in the direction of transport with an increasing energy regime. Cohesive sediments are more resistant to erosion by shear stress than non-cohesive sediments [Grabowski et al., 2011]. Specifically, sediment cohesion can affect the stability of the substrate. Adding clay to a sand bed makes it more resistant to erosions by smoothing the surface and by changing its mechanical properties [Grabowski et al., 2011]. Although cohesion may affect the sediment texture, all sample distributions were dominantly sand size, therefore cohesion should only be a minor consideration.

Another factor to consider is sediment trapping. Net sediment transport in a tide dominated environment depends on the scale and direction of the tidal residual flow [Wu et al., 2011]. Residual circulation forms a closed gyre in the western lower Bay of Fundy and could be a location for retention of fine sediments [Gelati, 2012]. Furthermore, net

accretion of sediment was recorded in Cobequid Bay, which was also attributed to sediment trapping and redistribution [Amos and Long, 1980]. Abundant sand dunes present near Cape Chignecto reflect an imbalance between sediment supply and current velocity, in that the sediment is confined by the overall net transport into the Bay [Todd et al., 2014]. The Scots Bay dune field is located at the site of a large gyre [Shaw et al., 2012]. Strong flows entering the Minas Passage during the flood tide are reflected by the gravels dunes located on the north shores. This is coupled with a weaker westward flow along the south shoreline and the absence of gravel dunes [Shaw et al., 2012]. Therefore it appears that sediment input is greater than sediment output in the Minas Passage. Lastly, a seasonal variation of the frequency of storms could affect sediment availability, in that cliffs are eroded the most during storms.

5.2.4 Where is sediment texture in hydrodynamic equilibrium?

The previous discussion provides many instances where hydraulic stresses are not reflected in the sediment texture. However, a well-documented sedimentary environment where sediment texture and distribution in agreement with energy is on continental shelves [Swift et al., 1971, Gelati, 2012, Gamberi et al., 2014]. For example, Gelati's [2012] predictions of competent mean grain size are in better agreement with observed in the Gulf of Maine. Relict sediments on shelves have been defined as a remnant from a different earlier environment which can be recognized by petrographic, fauna, and topographic differences to modern sediment [Swift, 1971]. Relict sediments thus represent sediments which are no longer in equilibrium with modern environment. They were transported and deposited when the environment was different but are still subject to reworking and modification from the modern environment [Swift, 1971].

The geomorphology of continental shelves records present-day conditions, as well as past sea-level stages [Gamberi et al., 2014]. Relict sediments would be best preserved along tectonically inactive margins, such as that off the coast of Nova Scotia and northeastern USA. Gamberi et al. [2014] interpreted that sediment flux and reworking were negligible processes over long term periods to the sediments on the shelf offshore northeast. And were thus able to record preservations of past landscapes that show coastal settings different to present-day. Similarly, across the southern Californian shelf, sediment distribution and thickness are primarily controlled by sea level rise, as well as changes to sediment supply [Klotsko et al., 2015]. The shelf exhibited three deposition units, each recording a different interplay between rate of sea level rise and sediment supply [Klotsko et al., 2015].

The concept of continental shelves in a hydrodynamic equilibrium is often used and taught in sequence stratigraphy. The terms transgressive and regressive infer changes to continental shelves based on changes in sea-level, in that the sediments respond to changes in hydrodynamics. Relict sediments are found on open continental shelves, similar to the environment of the Gulf of Maine. This environment provides more suitable characteristics for use of hydrodynamic equilibrium concepts, than those within the Minas Basin.

5.3 Sediment transport and texture of the Minas Basin- Implications for tidal power development

Since seabed sediment texture is controlled by the texture from the eroding cliffs, it is unlikely that changes in energy from the installation of in-stream tidal turbines will affect the seabed grain size distribution. Sediments along the immediate coast are mobilised more frequently by strong wave shear velocities than tidal velocities (Li et al., 2015). Since

the cliffs erode independent of tidal energy, the grain sizes entering the Basin will remain the same. Ashall et al. [2016] developed a 3D hydrodynamic and sediment model of the Minas Basin to determine the implications of suspended sediment dynamics in the Minas Basin. After installation of turbine array, there was a local loss of energy, accompanied by a loss of bottom friction. Maximum tidal power extraction had a large impact on the suspended sediment concentration, reducing fine sediment mobilisation and increasing deposition on the tidal flats in Cobequid Bay. Depth and location averaged suspended sediment concentration (SSC) indicated that implementation of low and high tidal power extraction turbines would cause a 5.6 and 37% decrease in SSC, respectively [Ashall et al., 2016]. Although the magnitude of suspended sediment concentration might change, the texture will remain the same because the cliffs erode independent of tidal power. Since the texture is predicted to remain the same, the abundance and diversity of benthic habitats will not be affected. However, since sediment transport is dominated by tides, changes in energy could cause a change in morphology of the seabed and this may affect the distribution of benthic organisms within the Minas Basin.

Seabed geomorphology in tidal regimes changes over short timescales [Todd et al., 2014; Swift, 1968; Shaw 2012; Anthony, 2013]. Active sediment transport and deposition are common the Bay of Fundy System. Sand sheets can migrate tens of meters per year and sand dunes have been recorded to migrate 3 to 4.5 m in a month near Cape Spencer [Todd et al., 2014]. Since the geomorphology of seabed in the Basin is very dynamic, benthic organisms are already capable of adapting to changes which would be similarly caused with an anthropogenic decrease in energy.

In summary, the implications of energy extraction on seabed sediment texture are predicted to be minimal. Since the input of sediment to the Basin is large, the texture can be defined by the texture of input rather than by energy of flows within the basin. Thus the benthic habitats associated with specific seabed sediment textures will likely be unaffected.

CHAPTER 6 CONCLUSIONS

6.1 Conclusions

The distribution of grain sizes was determined for cliff, beach, and till sediments along the coast of the Minas Basin and compared to the distribution of seabed sediment samples from the Minas Basin and Bay of Fundy. The following was concluded from this comparison:

1) An overall coarsening from cliff to deep-water sediment was observed. From this, it was interpreted that sediment derived from the eroding cliffs was the dominant supply of sediment to the Basin and that sediment transport within the Minas Basin is controlled by tidal energy.
2) Although sediment transport is dominated by tidal hydrodynamics, seabed sediment texture is controlled by the input from adjacent eroding sandstone cliffs. Thus, an abundant supply of sediment finer than the competent mean grain size is used to explain the disagreement between observed and competent mean grain size. Therefore models need to incorporate a sediment transport component, such as one by Wu et al., 2011.
3) Since sediment supply controls seabed texture, it is unlikely that the installation of tidal turbines will have a large effect on the size of sediments in the Basin. The

turbines may however, affect the sediment transport, and thus the seabed geomorphology.

6.2 Future Work

There are limitations to the approach of this thesis. As previously mentioned, it would be beneficial to investigate the cohesive properties of sediments at different tidal zones in the Minas Basin. Furthermore, an overall updated sediment budget would be useful to quantify cliff recession rates. This thesis does not investigate changes to seabed morphology on a long time scale after impacted by tidal development, as well as does not investigate preferred sediment texture for specific benthic habitats. Predictions of seabed shear stress and sediment transport patterns still do not exist for the entire Bay of Fundy [Wu et al., 2011].

Ultimately though, a sediment texture pattern from onshore to offshore has emerged using changes in statistics of grain sizes. This approach has long been used to infer sediment transport mechanisms. This thesis is an example that simple sediment studies are still useful and necessary in order to grasp the fundamental controls of sediment texture and transport within a system. Field observations are necessary in order to parameterise and test numerical models.

It is been customary to assume that fluid transport rate and particle suspension respond to each other in an empirical way, and one can be used to make predictions on the other. But it is likely that system equilibrium is much more complex than that. Bigger-picture, conceptual questions which need to be asked are how long does it take before a system will achieve equilibrium? And how is anthropogenic infrastructure effecting our

fundamental concept of equilibrium? Which is an important question because many river and coastal systems are influenced by humans in some way now.

Literature Cited

Amos, C.L., B.F.N. Long (1980), The sedimentary character of the Minas Basin, Bay of Fundy, *The Coastline of Canada.*, 80-10, 123-152.

Anthony, E.J., (2013), Storms, shoreface, morphodynamics, sand supply, and the accretion and erosion of coastal barriers in the southern North Sea, *Geomorphology.*, 199, 8-21.

Ashall, L.M., R.P. Mulligan, B.A. Law (2016), Variability in suspended sediment concentration in the Minas Basin, Bay of Fundy, and implications for changes due to tidal power extraction, *Coast Eng.*, 107, 102-115.

Baker, V.R., D.F. Ritter (1975), Competence of rivers to transport coarse bedload material, *Geol Soc Am Bull.*, 86, 975-978.

Brooks, D.A., M.W. Baca, Y.T. Lo (1999), Tidal circulation and residence time in a macrotidal estuary: Cobscook Bay, Maine, *Estu Coast Shelfs.,* 49, 647-665.

Buffington, J.M., D.R. Montgomery (1997), A systematic analysis of eight decades of incipient motion studies, with special reference to gravel-bedded rivers, *Water Resour Res.*, 33, 1993-2029.

Buffington, J.M., D.R. Montgomery (1999), Effects of on sediment supply on surface textures of gravel-bed rivers, *Water Resour Res.,* 35, 3523-3530.

Buzeta, M.I., (2014), Identification and review of ecologically and biologically significant areas in the Bay of Fundy, DFO, Can Sci Advis Sec Res Doc. 2013/065, vi + 59 p.

Daborn, G.R., C. Pennachetti (1979), Physical oceanographic and sedimentological studies in the Southern Bight of Minas Basin, *Proc N.S. Inst Sci.,* 29, 315-333.

Daidu F., (2013), Classifications, sedimentary features and facies associations of tidal flats, *J. Palaeogeography.,* 2, 66-80.

Dietrich, W.E., J.W. Kirchner, H. Ikeda, F. Iseya (1989), Sediment supply and the development of the coarse surface layer in gravel-bedded rivers, Department of Geology and Geophysics, and Energy Resources Group, Univeristy of California, California.

Ferrer-Boix, C., and M.A. Hassan (2014), Influence of the sediment supply texture on morphological adjustments in gravel-bed rivers, *Water Resour Res.*, 50, 7206-7230.

Friedman, G.M., (1967), Dynamic processes and statistical parameters compared for size frequency distribution of beach and river sands, *J Sediment Petrol.,* 37, 327-354.

Friedrichs, C.T., (2011), Tidal Flat Morphodynamics: A synthesis, Treatise on Estuarine and Coastal Science, Virginia Institute of Marine Science, 3, 137-170.

Folk, R., and W.C. Ward (1957), Brazos river bar: a study in the significance of grain size parameters, *J. Sediment Petrol.*, 27, 3-26.

Gamberi, F., M. Rovere, A. Mercorella, E. Leidi, G. Dalla Valle (2014), Geomorphology of the NE Sicily continental shelf controlled by tidal currents, canyon head incision and river-derived sediments, *Geomorphology.*, 217, 106-121.

Gelati, S., (2012), Modeling the impact on sediment texture of large-scale tidal power in the Bay of Fundy. M.Sc

Gill, A., (2005), Offshore renewable energy: Ecological implications of generating electricity in the coastal zone, *J Appl Ecol.*, 42, 605-615

Grabowski, R.C., I.G. Droppo, G. Wharton, (2011), Erodibility of cohesive sediment: The importance of sediment properties, *Earth-Science Rev.*, 105, 101-120.

Hasegawa, D., J. Sheng, D.A. Greenberg, K.R. Thompson (2011), Far-field effects on tidal energy extraction in the Minas Passage on tidal circulation in the Bay of Fundy and Gulf of Maine

Hickin, E., (1995), Sediment Transport, *IAG Publ*, 44, 70-107.

Jackson, W.L., and R.L. Bechsta (1984), Influences of increased sand delivery on the morphology of sand and gravel channels, *Water Resour Res.*, 20, 527-533.

Karsten, R.H., M. McMillan, M.J. Lickley, R.D. Haynes (2008), Assessment of tidal current energy in the Minas Passage, Bay of Fundy, *P I Mech Eng A-J Pow.*, 222, 493-507.

Keppie, J.D. (compiler) 2000: Geological Map of the Province of Nova Scotia; Department of Natural Resources, Minerals and Energy Branch, Map ME 2000-1, scale 1:500 000.

Klotsko, S., N. Driscoll, G. Kent, D. Brothers (2015), Continental shelf morphology and stratigraphy offshore San Onofre, California: The interplay between rates of eustatic change and sediment supply, *Mar Geol.*, 369, 116-126.

Lambiase, J.J., (1980), Hydraulic control of grain-size distributions in a macrotidal estuary, *Sedimentology.*, 27, 433-446.

Li, M.Z., C.G. Hannah, W.A. Perrie, C.C.L. Tang, R.H. Prescott, D.A. Greenberg (2015), Modelling seabed shear stress, sediment mobility and sediment transport in the Bay of Fundy, *Can J. Earth Sci.*, 52, 757-775.

Lisle, T.E., F. Iseya, H. Ikeda, (1993), Response of a channel with alternate bars to a decrease in supply of mixed-sized bedload: A flume experiment, *Water Resour Res*, 29, 3623-3629.

McLaren, P., (1984), An interpretation of trends in grain size measures, *J. Sediment Petrol.*, 51, 611-624.

Methratta E.T., and J.S. Link (2006), Associations between surficial sediments and groundfish distributions in the Gulf of Maine-Georges Bank Region, *North American Journal Fish Mang*, 26, 473-489.

Neill, S.P., E.J. Litt, S.J. Couch, A.G. Davies (2009), The impact of tidal stream turbines on large-scale sediment dynamics, *Renew Ener*, 34, 2803-2812.

Peer, D.L., (1980), A review of benthic macro faunal production of the upper Bay of Fundy intertidal area, Marine Ecology Laboratory, Bedford Institute of Oceanography, 105-113.

Poiner, I.R., and R. Kennedy (1984), Complex patterns of change in the macrobenthos of a large sandbank following dredging, *Mar Biol.*, 78, 335-352.

Porter-Smith, R., P.T. Harris, O.B. Andersen, R.Coleman, D. Greenslade, C.J. Jenkins (2004), Classification of the Australian continental shelf based on predicted sediment threshold exceedance from tidal currents and swell waves, *Mar Biol.*, 211, 1-20.

Pritchard, D., and A.J. Hogg (2003), Cross-shore transport and the equilibrium morphology of mudflats under tidal currents, *J. Geophys Res.*, 108, 1-15.

Proosdij D. Van, J. Ollerhead, R. G. D. Davidson-Arnott (2000), Controls on suspended sediment deposition over single tidal cycles in a macrotidal saltmarsh, Bay of Fundy, Canada, *Geol Soc Spec Publ*, 175, 43-57.

Shaw, J., B.J. Todd, M.Z. Li, Y. Wu (2012), Anatomy of the tidal scour system at Minas Passage , Bay of Fundy , Canada, *Mar Geol.*, 323-325, 123-164.

Swift, D.J.P., (1968), Coastal erosion and transgressive stratigraphy, *J. Geol.*, 76, 444-456.

Swift, D.J.P., (1971), Relict sediments on continental shelves: A reconstruction, *J. Geol.*, 79, 322-346.

Todd, B.J., J. Shaw, M.Z. Li, V.E. Kostylev, Y. Wu (2014), Distribution of subtidal sedimentary bedforms in a macrotidal setting: The Bay of Fundy, Atlantic Canada, *Cont Shel Res.*, 83, 64-85.

Wu, Y., J. Chaffey, D.A. Greenberg, K. Colbo, P.C. Smith (2011), Tidally-induced sediment transport patterns in the upper Bay of Fundy: A numerical study, *Cont Shel Res.*, 31, 2041-2053.

Tanner, W.F. (1995), Environmental clastic granulometry, *Florida Geological Survey, Special Publication.*, 40, 142 pp.

Yeo, R.K., and M.J. Risk (1979), Intertidal Catastrophes: Effect of Storms and Hurricanes on Intertidal Benthos of the Minas Basin, Bay of Fundy, *J Fish Res Board Can.,* 36, 667-669.

Zhou, Z., G. Coco, M. Wegen, Z. Gong, C. Zhang, Ian. Townend (2014), Modeling sorting dynamics of cohesive and non-cohesive sediments on intertidal flats under the effect of tides and wind waves, *Cont Shel Res.,* 104, 76-91.

Appendix

Sample	Location		Retained Weight (g) on sieve (phi)																	
	Longitude	Latitude	-1.0	0.0	0.2	0.5	0.7	1.0	1.2	1.5	1.7	2.0	2.2	2.5	2.7	3.0	3.2	3.5	3.7	4.0	4.6
C01	-63.9872	45.39958	13.063	2.935	1.226	2.037	2.475	3.049	2.904	4.210	4.012	4.740	4.765	4.417	5.462	7.635	6.120	9.026	8.981	8.307	45.468
B01	-63.9872	45.3996	40.408	17.190	4.105	5.829	8.809	12.905	15.985	19.712	14.404	9.255	3.634	1.454	0.781	0.540	0.226	0.211	0.165	0.123	0.847
C02	-63.9844	45.39953	2.528	3.353	1.484	2.731	3.985	5.477	6.091	8.163	8.782	11.250	11.673	10.569	10.840	11.325	6.803	10.818	11.147	7.374	14.830
C03	-63.7818	45.3949	0.000	0.276	0.314	0.652	0.840	0.949	1.133	1.598	2.164	3.183	4.047	4.689	8.821	14.953	9.744	17.519	14.995	14.200	49.457
B03	-63.7818	45.39492	7.293	3.502	1.594	3.142	5.023	7.552	10.163	17.351	17.913	18.466	12.676	8.166	8.123	7.306	4.677	4.428	3.251	2.474	16.449
T03	-63.7818	45.39493	8.940	5.414	1.775	2.321	2.820	3.059	2.960	4.013	4.204	5.314	6.137	5.542	6.739	8.407	6.327	9.847	11.735	13.726	205.162
C05	-63.9194	45.36205	0.000	0.119	0.058	0.218	0.641	1.553	2.399	4.160	6.452	12.827	20.878	22.242	23.708	21.766	9.676	10.715	7.145	5.622	23.851
B05	-64.9194	46.36205	17.331	5.780	1.965	3.097	4.755	6.828	7.605	11.573	12.623	16.901	16.517	11.348	8.852	6.161	3.221	2.894	2.023	1.565	11.088
T05	-65.9194	47.36205	15.147	6.374	1.823	2.738	3.598	4.133	4.716	5.947	6.144	8.177	8.040	7.086	8.170	8.793	5.952	8.793	9.718	13.689	191.796
C06	-63.9198	45.36262	0.000	0.104	0.044	0.065	0.132	0.216	0.391	0.544	0.837	1.542	2.250	3.585	7.539	10.668	6.543	5.860	3.985	4.107	84.057
B06	-64.9198	46.36262	1.899	0.711	0.198	0.276	0.345	0.454	0.686	1.113	1.633	3.100	4.901	6.513	10.936	18.061	11.428	17.384	13.123	11.102	36.392
T06	-65.9198	47.36262	0.417	0.448	0.239	0.403	0.638	0.796	0.935	1.330	1.547	2.556	3.798	4.363	6.505	9.125	7.100	10.102	11.990	18.344	174.248
C07	-63.7818	45.3949	75.211	29.732	7.094	7.192	6.914	5.936	4.399	3.672	2.466	2.307	1.989	1.472	1.522	1.501	1.075	1.111	0.995	0.936	9.103
T08	-63.782	45.39772	91.624	22.544	5.636	6.566	6.355	5.375	3.877	3.286	2.310	2.214	1.874	1.403	1.347	1.529	1.032	1.083	1.083	1.061	9.256
C09	-63.7017	45.38977	0.111	1.428	1.001	1.546	2.069	2.028	2.319	1.564	1.970	2.534	2.549	2.134	2.537	2.808	2.413	3.598	5.587	9.963	108.583
C AR2	AR	AR	6.108	11.789	4.002	4.588	4.502	3.813	3.262	3.677	2.921	3.313	3.044	2.664	3.055	3.711	2.985	4.416	4.714	6.373	84.083
C AR3	AR	AR	22.550	9.570	3.583	4.436	4.688	4.564	4.213	4.960	4.200	4.979	4.936	4.184	5.098	5.531	3.899	5.480	5.433	5.313	102.401
C AR4	AR	AR	13.833	4.204	1.948	2.539	3.028	3.227	3.049	3.932	3.587	4.430	4.403	3.956	4.555	5.235	4.142	6.108	6.417	6.431	100.587
C AR6	AR	AR	8.608	6.136	2.529	3.295	3.739	3.971	3.752	5.042	4.476	5.624	5.816	5.646	6.378	8.132	5.930	8.310	7.770	7.204	122.435
C AR7	AR	AR	14.138	5.483	2.792	3.678	4.519	4.535	4.340	5.383	4.704	5.690	5.676	4.900	5.619	6.962	5.001	6.903	7.246	7.185	123.812
C10	-64.3433	45.25979	0.000	0.089	0.373	1.436	2.385	3.123	3.316	4.735	5.106	8.263	10.592	10.491	13.766	16.618	9.052	11.375	7.035	3.988	30.988
B10	-64.3433	45.25979	0.180	1.164	1.781	4.265	9.195	11.724	16.124	19.121	16.895	19.009	15.529	11.338	11.994	13.165	7.127	11.138	10.477	9.505	34.800
C11	-64.3451	45.25894	0.329	1.712	0.623	0.871	0.962	0.977	1.252	1.823	2.999	5.954	8.982	9.678	13.201	15.759	8.936	11.253	7.272	5.245	39.054

B11	-64.3452	45.25895	0.153	0.132	0.227	0.794	1.614	2.443	6.318	10.173	12.608	18.747	20.549	17.083	19.846	17.484	7.568	8.955	6.735	4.798	29.636
C12	-64.347	45.258	0.000	0.079	0.111	0.344	0.574	0.792	1.853	3.257	4.368	8.984	19.094	30.115	36.304	31.100	10.475	16.226	8.029	4.831	27.524
B12	-64.347	45.25801	0.260	0.292	0.474	1.585	3.249	5.979	7.024	9.126	9.250	14.187	14.847	13.857	16.057	16.552	8.296	10.123	6.901	5.697	30.492
C13	-64.3487	45.25712	0.000	0.593	0.330	0.537	0.653	0.882	1.330	1.845	2.084	3.029	3.378	3.569	4.419	6.527	5.487	10.012	10.576	12.415	84.687
B13	-65.3487	45.25713	0.341	0.390	0.588	1.324	2.188	3.291	5.078	7.625	8.762	13.418	15.897	14.082	15.640	16.171	9.925	11.000	7.168	5.341	21.757
C14	-64.3504	45.25624	0.043	0.349	0.268	0.394	0.532	0.638	0.674	0.721	0.702	0.883	0.916	0.969	1.291	2.098	2.580	4.356	5.986	8.659	150.033
B14	-64.3504	45.25625	1.413	2.627	2.745	4.768	6.958	10.275	11.089	12.775	12.570	17.204	17.716	12.980	13.668	13.230	6.668	8.228	7.457	6.457	27.279
C15	-64.3559	45.24103	0.000	0.995	1.358	2.719	3.190	3.309	3.474	5.011	5.127	6.856	7.848	7.556	10.716	14.563	8.565	14.675	11.878	9.798	31.727
C16	-64.355	45.24231	0.000	0.146	0.307	1.021	2.247	3.051	4.445	5.810	5.752	6.986	7.967	6.846	8.342	9.818	6.857	10.227	8.355	7.815	42.544
B16	-64.355	45.24232	2.668	0.480	0.816	2.096	4.460	6.860	12.059	16.229	14.112	15.716	15.828	14.788	17.578	16.386	7.790	8.973	5.863	4.400	14.957
B17	-64.3549	45.24364	2.156	5.647	4.047	5.729	6.377	6.502	8.851	11.116	10.659	15.342	22.750	30.077	26.590	25.764	8.419	11.972	7.882	6.091	24.188
C18	-64.3548	45.245	0.000	0.000	0.000	0.054	0.195	0.699	4.601	5.715	4.273	4.625	4.189	3.105	4.188	5.229	4.067	6.949	7.491	10.091	83.144
B18	-64.3548	45.24501	9.511	2.010	2.657	5.503	9.099	10.710	13.638	15.340	11.650	10.504	7.936	4.891	5.234	4.991	3.544	4.144	3.974	3.779	29.698
C19	-64.3547	45.24643	0.162	1.408	1.124	1.983	2.661	2.820	3.595	4.767	3.457	3.189	2.360	1.794	1.997	2.492	2.439	3.532	4.694	5.981	117.977
B19	-64.3547	45.24644	25.500	2.662	2.449	4.369	5.916	7.666	8.629	10.879	9.076	10.068	10.502	8.941	11.263	11.435	6.229	7.751	6.394	6.510	66.060
T19	-64.3547	45.24645	37.034	0.230	0.170	0.479	1.091	2.329	3.234	4.146	3.610	3.899	3.889	3.462	3.878	4.820	3.683	5.412	5.313	6.108	92.774
C20	-64.3546	45.24803	0.000	0.016	0.057	0.193	0.424	0.809	2.431	3.475	2.576	2.345	1.617	1.180	1.369	1.922	2.118	3.782	5.445	8.377	163.412
B20	-64.3546	45.24804	19.851	0.126	0.344	1.330	3.048	6.649	10.674	16.984	15.878	17.159	13.980	10.078	9.925	8.620	5.275	5.736	4.884	4.629	47.825
T20	-64.3546	45.24805	0.000	0.039	0.109	0.368	0.872	1.956	3.363	5.271	5.717	7.381	8.342	7.825	10.922	14.399	8.466	13.652	9.930	8.784	45.947
C21	-64.3534	45.24928	0.000	0.085	0.101	0.267	0.461	0.855	1.557	3.129	3.575	4.608	5.094	5.243	6.668	9.456	6.326	10.620	9.658	9.427	64.693
B21	-64.3534	45.24929	0.668	0.177	0.321	1.046	2.434	5.559	9.339	15.540	15.607	17.555	15.824	11.975	13.448	14.841	8.065	9.569	7.391	6.022	41.499
C22	-64.3526	45.25054	0.000	0.009	0.110	0.586	1.865	3.999	10.310	13.275	9.260	8.495	6.505	4.651	4.657	4.479	3.240	3.454	3.391	3.434	66.986
B22	-64.3526	45.25055	0.947	0.025	0.054	0.233	1.802	4.766	8.678	13.448	12.346	13.423	10.227	8.128	7.765	8.074	5.621	8.471	8.844	9.972	74.196
C23	-64.3525	45.25205	0.000	0.019	0.096	0.424	1.309	3.173	6.405	10.231	8.220	8.518	7.534	6.237	7.409	8.403	6.288	7.411	7.045	6.845	93.942
B23	-64.3525	45.25206	0.138	0.219	0.481	1.846	4.130	9.725	13.896	17.555	14.528	14.545	13.814	12.584	13.766	15.253	7.093	9.184	7.794	7.528	70.738
C24	-64.3521	45.25348	0.002	0.024	0.034	0.067	0.102	0.125	0.155	0.171	0.179	0.230	0.299	0.529	1.106	2.195	2.714	4.726	6.856	10.302	158.093
B24	-64.3521	45.25349	0.559	0.410	0.697	2.171	5.285	13.577	18.394	22.151	18.696	17.494	14.476	15.731	22.706	25.241	9.794	14.821	10.028	8.679	60.736
C25	Blom	Blom	0.000	0.070	0.049	0.205	0.440	0.831	1.822	3.635	4.044	4.749	4.959	4.218	5.934	8.940	7.296	11.653	12.256	13.403	98.099
B25	Blom	Blom	0.037	0.492	0.352	0.836	1.693	2.797	4.311	7.014	7.834	12.796	19.530	22.618	25.488	25.528	9.787	14.817	10.516	9.176	45.217

T25	Blom	Blom	0.080	0.027	0.004	0.063	0.235	0.700	2.488	3.560	3.216	4.386	4.742	4.653	6.174	8.297	5.521	7.944	7.327	7.501	85.176
C26	-64.2305	45.10977	0.000	0.216	0.270	0.733	1.505	2.442	8.097	19.264	15.155	13.996	10.278	7.076	6.958	6.409	4.517	4.273	3.521	3.097	70.323
B27	-64.2283	45.10961	9.588	2.120	1.506	2.898	4.085	5.164	15.373	19.541	13.750	12.803	9.634	6.466	5.666	4.766	3.028	2.708	2.209	1.942	50.850
C28	-64.2264	45.10925	0.035	1.587	1.509	2.762	4.024	5.088	15.962	19.587	12.434	10.518	7.686	5.343	5.224	4.800	3.582	3.304	2.816	2.448	62.768
B28	-64.2264	45.10926	3.071	3.974	2.511	3.930	4.563	4.899	8.357	14.028	9.902	9.210	6.936	4.879	4.870	4.475	3.207	3.189	2.814	2.593	60.560
B29	-64.2246	45.10879	0.662	10.435	5.648	7.182	7.644	7.280	6.343	10.364	11.243	12.073	8.327	5.460	4.999	4.559	2.986	2.962	2.569	2.506	50.357
C30	-64.2233	45.10773	0.616	6.622	3.841	5.209	5.784	6.129	11.571	13.419	9.607	9.482	7.344	5.887	8.618	7.758	0.578	2.550	3.188	2.677	55.978
B30	-64.2233	45.10774	4.173	4.995	2.665	3.449	3.740	3.961	11.226	16.112	11.267	11.073	8.308	5.872	5.804	5.494	4.046	3.856	3.381	3.199	73.796
C31	-64.2214	45.10727	0.575	7.995	3.052	3.241	3.016	2.794	2.426	3.192	9.026	14.131	10.608	7.225	6.620	6.052	4.022	3.934	3.293	2.977	78.996
B31	-64.2215	45.10728	0.806	8.946	5.396	7.096	7.559	6.775	5.539	6.216	9.897	14.746	10.653	6.821	6.258	5.452	3.804	3.798	3.688	3.080	69.059
B32	-64.22	45.10629	3.653	3.498	4.884	9.517	12.193	11.884	11.847	13.176	8.580	7.349	5.335	3.629	3.584	3.260	2.633	2.279	2.084	2.236	46.057
C33	-64.2192	45.10516	0.331	6.623	3.553	3.545	4.228	4.119	10.768	16.582	11.156	10.115	7.524	5.341	5.116	4.863	3.591	3.327	3.020	2.504	60.948
B34	-64.2183	45.10386	21.426	10.557	2.838	3.012	2.875	2.953	6.888	12.459	9.254	8.659	6.622	4.709	4.748	4.374	3.504	3.091	2.831	2.950	69.871
B35	-64.2173	45.10283	5.016	3.001	2.756	4.873	5.630	5.720	9.954	16.059	11.130	9.785	6.965	4.751	4.492	4.079	2.880	2.749	2.309	2.045	47.325
B36	-64.2161	45.10017	52.165	6.884	3.038	3.168	3.428	3.383	5.561	8.862	6.090	5.662	4.241	2.931	2.950	2.777	2.299	1.969	1.630	1.599	33.110
C37	-64.215	45.09898	0.416	4.929	2.060	2.683	3.040	3.165	13.263	17.676	11.460	10.080	7.492	5.260	5.285	4.945	3.772	3.477	2.915	2.516	65.327
B38	-64.2138	45.09793	8.754	13.660	6.818	8.456	9.387	9.563	12.529	14.441	9.072	7.805	5.753	3.894	3.777	3.298	2.438	2.091	1.725	1.453	35.562
C39	-63.8061	45.29607	10.007	7.623	1.915	2.230	2.394	2.751	2.650	3.413	3.361	4.250	4.368	3.839	4.029	4.275	3.324	3.448	3.390	2.412	44.835
C40	-63.8073	45.29705	6.594	2.121	0.784	1.247	1.594	2.097	2.305	2.367	3.644	4.854	5.340	4.890	4.939	5.259	3.932	3.852	3.420	2.858	39.729
C41	-63.8084	45.29795	3.400	5.304	1.686	2.113	2.422	2.582	2.456	3.114	3.067	3.879	3.916	3.371	3.644	3.798	3.003	3.191	2.940	3.385	39.111
C42	BCH	BCH	0.360	4.766	5.949	11.814	13.156	11.797	9.380	8.872	5.972	5.184	4.038	3.147	3.309	3.109	2.079	1.724	1.229	0.797	5.521
C43	-63.8098	45.29858	28.487	12.279	3.704	4.712	5.054	5.259	4.842	5.470	4.065	3.358	2.042	1.237	1.133	1.004	0.751	0.755	0.607	0.463	8.595
C44	-63.8129	45.29952	23.820	24.636	7.591	8.432	8.031	6.334	4.534	3.760	2.531	2.133	1.339	0.732	0.527	0.273	0.155	0.128	0.107	0.081	11.374
C45	-63.8131	45.30062	5.255	20.050	5.172	6.277	6.430	5.987	4.560	5.203	4.344	4.948	4.318	3.081	2.373	1.424	0.615	0.470	0.330	0.258	34.497
C46	-63.8137	45.30187	14.606	22.797	6.464	7.723	8.036	7.222	5.581	5.213	3.585	3.427	2.727	1.921	1.928	1.663	1.121	1.081	0.834	0.607	6.379
C47	-63.8121	45.30305	63.510	9.744	1.781	1.969	2.070	2.106	1.977	2.710	2.812	3.650	3.123	2.128	1.816	1.196	0.670	0.554	0.413	0.320	10.544
C48	-63.8113	45.30408	23.564	16.392	3.703	5.079	5.745	5.911	5.201	5.101	3.391	3.222	2.497	1.774	1.709	1.334	0.870	0.759	0.554	0.385	5.263
C49	-63.8125	45.30545	41.318	11.471	3.048	3.295	3.899	4.215	3.805	4.390	3.529	3.357	2.354	1.527	1.390	1.193	0.831	0.776	0.604	0.497	6.713
C50	-63.8117	45.30673	4.489	7.805	2.313	3.184	3.634	4.215	4.170	6.292	6.309	7.454	6.459	4.573	3.633	2.350	1.096	0.646	0.360	0.227	10.885

C51	-63.8108	45.30785	4.489	7.805	2.313	3.184	3.634	4.215	4.170	6.292	6.309	7.454	6.459	4.573	3.633	2.350	1.096	0.646	0.360	0.227	10.885
C52	-63.8089	45.30873	22.351	11.199	1.973	2.016	1.984	1.906	1.799	2.169	2.354	3.002	3.412	3.026	3.459	3.576	2.671	2.662	2.227	1.878	32.192
C53	-64.1857	45.10102	11.293	4.764	1.149	1.403	1.419	1.395	1.295	1.717	1.759	2.292	2.357	2.115	2.478	2.741	2.497	3.181	3.312	3.112	54.519
C54	-64.1842	45.09935	22.356	6.869	1.678	1.875	2.215	2.318	2.132	2.709	2.392	2.873	2.722	2.306	2.517	2.514	2.131	2.381	2.162	1.720	34.065
C55	-64.1834	45.09872	18.041	11.287	2.156	1.827	2.251	2.188	1.932	2.309	1.998	2.284	2.094	1.656	1.811	1.919	1.582	1.793	1.627	1.241	32.825
C56	-64.1892	45.15517	1.286	1.487	0.517	0.636	0.637	0.570	0.377	0.485	0.494	0.598	0.599	0.582	0.569	0.874	1.200	2.682	5.124	8.782	62.529
C57	-64.1897	45.15477	40.714	14.711	2.495	2.271	2.145	1.915	1.382	1.680	1.418	1.645	1.526	1.486	1.491	1.562	1.259	1.348	1.186	1.010	20.611
C58	-64.191	45.15287	67.820	17.606	2.331	2.003	1.653	1.356	0.955	0.950	0.741	0.738	0.597	0.488	0.523	0.462	0.327	0.368	0.313	0.269	1.878
C59	-64.1671	45.16398	28.269	13.790	2.723	2.513	2.355	2.147	1.665	1.946	1.605	1.745	1.543	1.377	1.465	1.429	1.143	1.255	1.060	0.853	30.098
C60	-64.1672	45.16325	27.984	7.011	1.658	1.817	1.934	2.000	1.824	2.333	2.110	2.475	2.180	1.819	2.124	2.050	1.746	2.015	2.153	2.158	37.211
C61	-64.1149	45.21035	16.503	5.766	0.774	0.732	0.642	0.562	0.375	0.396	0.308	0.334	0.272	0.219	0.230	0.194	0.150	0.158	0.131	0.133	0.856